Distribution Agreement

In presenting this thesis as a partial fulfillment of the requirements for a degree from Emory University, I hereby grant to Emory University and its agents the non-exclusive license to archive, make accessible, and display my thesis in whole or in part in all forms of media, now or hereafter now, including display on the World Wide Web. I understand that I may select some access restrictions as part of the online submission of this thesis. I retain all ownership rights to the copyright of the thesis. I also retain the right to use in future works (such as articles or books) all or part of this thesis.

Stephanie Phillis April 15th, 2013

The Number of Membranous Organelles in Mutant and Wild-type *C. elegans* Spermatids

by

Stephanie Phillis

Dr. Steven L'Hernault
Adviser

Department of Biology

Dr. Steven L'Hernault

Adviser

Dr. William Kelly

Committee Member

Dr. Guy Benian

Committee Member

2013

The Number of Membranous Organelles in Mutant and Wild-type *C. elegans* Spermatids

By

Stephanie Phillis

Dr. Steven L'Hernault

Adviser

An abstract of
a thesis submitted to the Faculty of Emory College of Arts and Sciences
of Emory University in partial fulfillment
of the requirements of the degree of
Bachelor of Sciences with Honors

Department of Biology

2013

Abstract

The Number of Membranous Organelles in Mutant and Wild-type *C. elegans* Spermatids
By Stephanie Phillis

During *C. elegans* spermatogenesis, fibrous body membranous organelles (FB-MOs) are present through the developmental progression from syncytial pachytene spermatocytes to spermatids (L'Hernault, 2009). FB-MOs contain major sperm protein, which is required for spermatozoan motility, plus other proteins needed for successful fertilization, making them a crucial part of functional sperm development. FB-MOs consist of three major parts, a membranous organelle (MO) head, a collar region separating the MO head from the fibrous body, and a fibrous body (FB) that contains major sperm protein filaments. In developing spermatids, the FB compartment disassembles releasing depolymerized major sperm protein dimers into the spermatid cytoplasm. After FB disassembly, the MO assumes a position beneath the plasma membrane. During spermiogenesis (the transition of a spermatid into a spermatozoon) the head fuses with the spermatozoon plasma membrane, releasing its contents and creating permanent fusion pores. The exact influence that FB-MOs have on the asymmetrical divisions of spermatogenesis and the development of fertilization competence by sperm is still incompletely understood. My thesis uses a vital staining technique to examine MO number and physiology and whether it is affected in various diverse *spe*rmatogenesis-defective (*spe*) mutants. This vital staining technique requires that MOs have a function vacuolar (V-) ATPase to become acidified, so my work showed that certain mutants with defective MO structure had competent V-ATPase activity. Additionally, I correlated MO number and position was correlated with spermatid volume. I found that spermatid volume varies under certain conditions but that the number of MOs seems to scale with cell volume, suggesting that spermatids can "count" organelles. In the future, the mutant survey I initiated should be more widely applied as it seems to offer a robust way to identify defects in MO physiology and/or numerical/volume ratios.

The Number of Membranous Organelles in Mutant and Wild-type *C. elegans* Spermatids

By

Stephanie Phillis

Dr. Steven L'Hernault

Adviser

A thesis submitted to the Faculty of Emory College of Arts and Sciences
of Emory University in partial fulfillment
of the requirements of the degree of
Bachelor of Sciences with Honors

Department of Biology

2013

Acknowledgements

I would like to thank the Dr. Steven L'Hernault, Dr. Candice Elam, and Elizabeth Gleason for their unwavering support with this work. Additionally, I thank Drs. Steven L'Hernault and W.C. Lindsey for the use of their unpublished results on *spe-21*. This work was funded by grants from the National Institutes of Health, Hughes Foundation and Emory College.

Table of Contents

TABLES AND FIGURES

1. INTRODUCTION

Diploid germ cells (together referred to as germ lines) undergo cell differentiation (gametogenesis) to form haploid gametes. A male has a germline that completes spermatogenesis, and a female has a germline that completes oogenesis. The fusion between a sperm and an oocyte results in fertilization, and this is followed by embryonic development (Nishimura and L'Hernault, 2010).

In *C. elegans*, there are two sexes: male and hermaphrodite, which can be easily identified based on morphological differences in tail structure. Males have an XO karyotype, and hermaphrodites have an XX karyotype (Brenner, 1974). The male germline performs spermatogenesis, while the hermaphrodite germline first performs spermatogenesis and later performs oogenesis. The *C. elegans* hermaphrodite is therefore capable of reproducing either by self-fertility or cross fertility, should it mate with a male (Hirsh et al., 1976). Males occur spontaneously among the self-progeny of a hermaphrodite at a rate of one in 700 animals (Hodgkin, 1974). The genetics and gonad anatomy/physiology of *C. elegans* makes it a particularly useful model system for studying biological processes related to reproduction (Herman, 2005; Brenner, 1974). Hermaphrodites are optically transparent facilitating viewing in live animals and self-fertility allows for convenient strain maintenance without having to set up crosses. Males can be mated to hermaphrodites to transfer genetic markers and mutant genotypes for phenotypic studies (Brenner, 1974).

The physiology and cytology of *C. elegans* male germline functions are of great interest because several known spermatogenesis defective (*spe*) mutant genes are orthologs of mammalian genes (Nishimura and L'Hernault, 2010; L'Hernault, 1997). There are approximately 60 *spe* mutants that have been identified in *C. elegans* that directly affect sperm

production and function (L'Hernault 1997; L'Hernault and Singson, 2000). Consequently, further investigations of *spe* mutants in *C. elegans* will likely be useful in future understandings of mammalian fertility and spermatogenesis (Nishimura and L'Hernault, 2010).

2. REPRODUCTIVE ANATOMY OF THE HERMAPHRODITE

The *C. elegans* hermaphrodite is a modified female that is capable of sperm production during a brief period prior to oocyte production (Hirsh et al., 1976). The reproductive system of the hermaphrodite has three parts: the germ line, the somatic gonad, and the egg-laying apparatus (Altun and Hall, 2006). The germ line includes germ cells, oocytes, and sperm. The egg-laying apparatus includes the vulva, the uterus, various associated muscles, and local neuropil/egg-laying neurons (Altun and Hall, 2006). The hermaphrodite gonad has an overall arrangement that is two U-shaped tubular structures that meet at the centrally located vulva (Altun and Hall, 2006). Each U shaped structure has two arms, the distal arm on the dorsal side, and the proximal arm on the ventral side (Hirsch et al., 1976). The proximal arm connects to the spermatheca, the chamber into which eggs are ovulated and fertilized. Germ cells within the hermaphrodite gonad, like the male gonad, exist in syncytium in the distal arm through the central canal, called the rachis (Altun and Hall, 2006; Hirsh et al., 1976).

Germ cells within the distal arm have a circumferential arrangement, with their nuclei creating a peripheral ring around the cytoplasmic core of the tubular arm (Hirsh et al., 1976). Within the cytoplasm of the distal gonad, there are non-membrane bound ribosomes, many mitochondria, and few microtubules. Progressing through the hermaphrodite gonad toward the proximal arm, germ cells display distal-to-proximal polarity that is also seen in male germ lines. Mitotic cells are found in the area most distal from the loop, and there is a gradient of progressing meiotic cells moving proximally down the length of the arm (Hirsh et al., 1976;

Altun and Hall, 2006).

3. REPRODUCTIVE ANATOMY OF THE MALE

The male reproductive system can be divided into the somatic gonad, the germline, and the proctodeum. The male gonad is composed of a singular, J-shaped tubular structure (Klass et al., 1976). Unlike the hermaphrodite germline, the male germline only produces spermatids. However, similarly to the hermaphrodite germline, the male germline also has distal-to-proximal germ cell polarity (Hirsh et al., 1976; Klass et al., 1976; Kimble and Hirsh, 1979). Moving proximal from the distal terminus, which is the end of the shorter side of the J-shape, the male reproductive system includes the testis, distal tip cells, the germ line, the seminal vesicle, the valve region, the vas deferens, the cloaca, and the cloaca opening. Similar to the hermaphrodite, the 180° turn in the male gonad is referred to as the loop (Klass et al., 1976; Hodgkin, 1974). The distal arm of the J-shaped gonad is the shorter arm, located on the ventral side of the animal. Often, the distal arm is referred to as the testis (Chitwood and Chitwood, 1974; Wolf et al., 1978). The proximal arm is located on the dorsal side of the animal (Wolf et al., 1978). The rachis of the male germline lacks the "chains" of germ cells crossing its center that are visible in hermaphrodites. Rather, in males, the germ cells are strictly on the periphery of the germline (Morgan et al., 2010).

Within the first 100 μm of the proximal arm, more Golgi complexes and endoplasmic reticulum are present than in the distal arm (Wolf et al., 1978). Slightly more than 100 μm away from the loop, the cytoplasm of the rachis begins to have noticeable difference from the cytoplasm of the peripheral cells. The cytoplasm of the rachis in this region has endoplasmic reticulum and ribosomes, but lacks the Golgi complexes, mitochondria, and free ribosomes observed in the peripheral cytoplasm (Wolf et al., 1978).

Approximately 150 to 200 μm from the loop, bulbous special vesicles, now called the membranous organelles (see Ward et al., 1981), can be observed on the edges of Golgi complexes. On the side connected to the Golgi complex, the vesicles have narrow collars or necks. On the cytoplasmic side opposite to the connection to the Golgi complex, cisternae of the endoplasmic reticulum surround the vesicles (Wolf et al., 1978). Also in this region of the proximal arm, fibrous bodies can be observed nearby to Golgi complexes. A gradient of increased size is visible in the fibrous bodies when moving down the length of the proximal arm toward the cloaca. Both the special vesicles and the fibrous bodies are observed in the peripheral cytoplasm of the proximal arm, not the rachis (Wolf et al., 1978). About 275 μm from the loop, the rachis is no longer identifiable in the proximal arm, as multiple nuclei are spread throughout the tubular structure of the proximal arm. Finally, about 280 μm from the loop, germ cells commit to gametogenesis by beginning to undergo a series of two meiotic divisions (Wolf et al., 1978).

4. SPERMATOGENESIS

As previously explained, *C. elegans* hermaphrodites are capable of both sperm and oocyte production (Hirsh et al., 1976). The hermaphrodite germline functions initially as a testes, and it begins sperm production during the fourth larval stage of development. During maturation into an adult, the hermaphrodite germline switches from a testis to begin functioning as an ovary performing oogenesis. In males, spermatogenesis also begins at the fourth larval stage, but continues throughout adulthood (Hirsh et al., 1976; Ward and Carrel, 1979). For the purposes of this paper, the focus of the *C. elegans* germline functions will be on spermatogenesis.

C. elegans offer a number of advantages for studying spermatogenesis. Firstly, wild-type primary spermatocytes differentiate into spermatids in approximately 90 minutes, and are capable of doing so *in vitro* in a simple, chemically defined medium (Ward et al., 1981; L'Hernault and Roberts, 1995; Nelson and Ward, 1980; Machaca et al., 1996). Additionally, the transparent nature of *C. elegans* allows for easy light microscopic observation of sperm development and behavior either *in vivo* or *in vitro* (L'Hernault, 1997).

C. elegans sperm crawl using an extended pseudopod that has a complex cytoskeleton of filamentous polymers of Major Sperm Protein (MSP; Theriot, 1996). The physiology of spermatogenesis is very similar between males and hermaphrodites (Klass et al., 1976). For clarity, spermatogenesis refers to the process of developing sperm, sperm refers to all haploid male gametes, spermatids refers to haploid male gametes that have not yet undergone spermiogenesis (or activation that converts them to spermatozoa), and spermatozoa refers to fully mature haploid male gametes (Ward et al., 1981).

Spermatogenesis begins when germ cells complete mitotic proliferations and transition into meiotic divisions (Wolf et al., 1978; Ward et al., 1981). Germ cells along the periphery of the germline that share cytoplasm with the rachis begin closing their plasma membranes, and start meiosis. When germ cells finish budding from the rachis, they are completely surrounded by plasma membranes (and no longer a shared cytoplasm) and are referred to as primary spermatocytes (Ward et al., 1981; Klass et al., 1976; Wolf et al., 1978).

Primary spermatocytes are 4N and complete meiosis I to form two secondary spermatocytes with 2N nuclei (see Fig. 1) (Ward et al., 1981). In meiosis I, the chromatin condenses, and primary spermatocyte nuclei are divided with the traditionally observed spindle of microtubules (Ward et al., 1981). The division of primary spermatocytes to secondary

spermatocytes can occur with complete or incomplete cytokinesis, creating separate secondary spermatocytes, or two attached secondary spermatocytes, respectively. Attached secondary spermatocytes will continue to meiosis II by elongating in parallel, while separate secondary spermatocytes will continue differentiating without contact from other spermatocytes (Ward et al., 1981).

Secondary spermatocytes undergo meiosis II and bud from a central acellular body, called the residual body that forms between the dividing nuclei (Ward et al., 1981). The haploid gametes produced by meiosis II during spermatogenesis are called spermatids. There are two situations that can occur when secondary spermatocytes divide into spermatids. The first is that secondary spermatocytes disjoined completely during meiosis I and therefore have plasma membranes that are no longer connected to each other. In this instance, the residual body forms between the now two haploid nuclei during meiosis II, and eventually the two nuclei become compartmentalized into 2 spermatids. The second situation is that secondary spermatocytes did not completely disjoin during meiosis I, leaving secondary spermatocytes that share a plasma membrane entering meiosis II. In this instance, the residual body forms between the now four haploid nuclei during meiosis II, and eventually the four nuclei become compartmentalized into four spermatids (Ward et al., 1981). Spermatids have a spherical shape (Ward et al., 1981; Wolf et al., 1978). Meiosis II is rather rapid in secondary spermatocytes, lasting approximately 2 to 5 minutes. In meiosis I, nuclei are visibly seen dividing with spindles of microtubules and a conventional actin-mediated cytokinesis (Ward et al., 1981). Like meiosis I, meiosis II involves a spindle composed of microtubules. However, the budding of spermatids during meiosis II is not a conventional cytokinesis. Membrane forms between the spermatids and the residual body prior to budding (Ward et al., 1981). Interestingly, no contractile ring, microtubules, or

microfilaments have been observed that could plausibly drive the budding of spermatids from the residual body, as one would expect during conventional animal cell cytokinesis. Somehow, the budding process involves actin filaments because the *spe*-15 gene, which encodes a myosin 6, is required for this process (Kelleher et al., 2000). The budding of spermatids from the residual body seems to resemble that of plant cell cytokinesis (Ward et al., 1981; O'Brien et al., 1969; Yamada, 1957).

The division of the cytoplasm and intracellular components during meiosis II is asymmetrical (Ward, 1986). After the budding of spermatids, the Golgi complex, the endoplasmic reticulum, actin, myosin, tubulin and ribosomes are partitioned into the residual body (Ward, 1986). The spermatid contains a haploid nucleus, a centriole pair, mitochondria, laminar membranes of unknown origin and previously mentioned special vesicles and fibrous bodies (Ward, 1986; Wolf et al., 1978). Since it naturally lacks ribosomes, spermatids must complete maturation into spermatozoa in the absence of new protein synthesis.

In the hermaphrodite, spermatids are pushed into the spermatheca during the first ovulation. In the spermatheca, spermatids undergo spermiogenesis, or activation, and become mature spermatozoa. Spermatozoa remain in the spermatheca in the hermaphrodite to fertilize incoming oocytes that enter during ovulation (Ward and Carrel, 1979). In the male, spermatids accumulate in the seminal vesicle, and remain there until ejaculation. Male-derived spermatids only undergo spermiogenesis during ejaculation when there is exposure to seminal fluid (Ward and Carrel, 1979). In general, sperm from males are significantly larger than those from hermaphrodites (LaMunyon and Ward, 1995; LaMunyon and Ward, 1998).

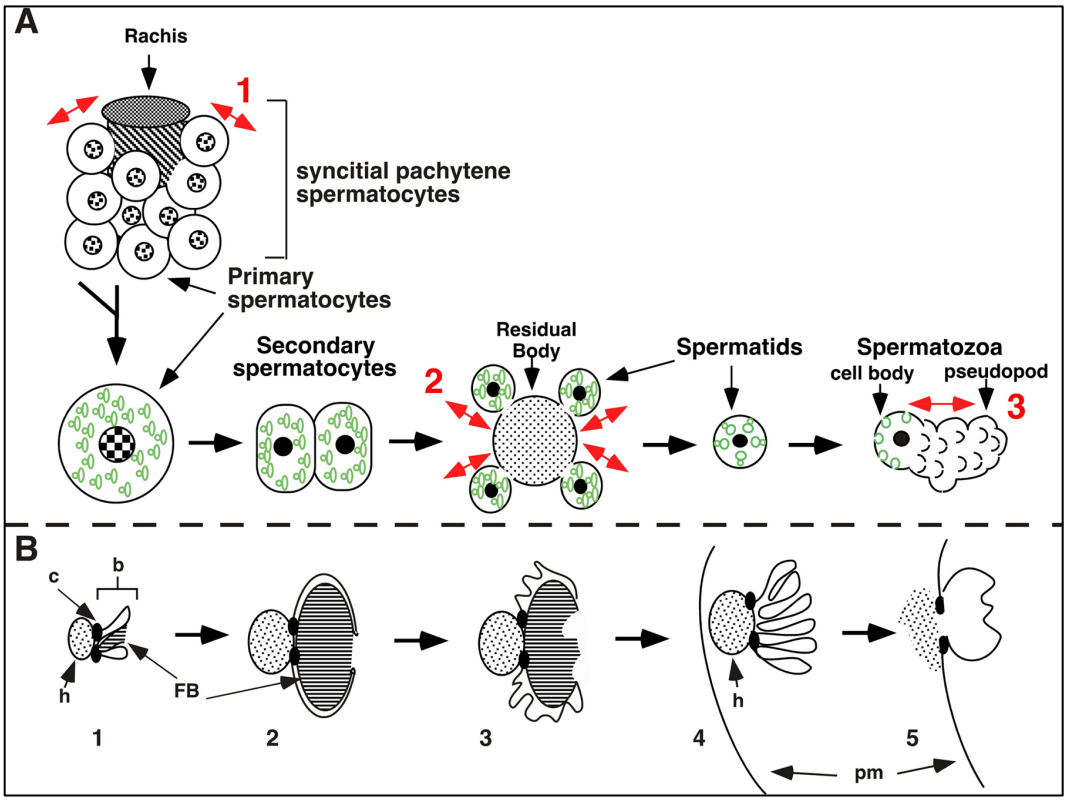

Fig. 1 (A) Summary of spermatogenesis. **(B)** Summary of FB-MO complex morphology and behavior during spermatogenesis. 1: FB becomes closely associated and then engulfed by the MO in primary spermatocytes. 2: General FB-MO complex structure. The smaller oval to the left is the MO, the collar is the noose-like constriction between the two ovals, and the FB is the larger, darkly shaded oval on the right. 3: MO degradation and FB MSP fiber depolymerization. 4: MO localization near the spermatid plasma membrane. 5: MO fusion to the plasma membrane as part of spermiogenesis. Figure originally from: L'Hernault, S.W. 2006. Spermatogenesis *WormBook*, ed. The *C. elegans* Research Community, WormBook, doi/10.1895/ wormbook.1.85.1, http://www.wormbook.org.

5. FB-MOS

During spermatogenesis, the presence of fibrous bodies (FBs) and membranous organelles (MOs) (previously referred to as special vesicles), which combine to form FB-MO complexes, are thought to influence the division of cytoplasm (Wolf et al., 1978; Ward et al., 1981). MOs are first observed nearby the Golgi complex, when spermatocytes have not yet individualized from the rachis cytoplasm, and are still in the pachytene stage (Wolf et al., 1978; Ward et al., 1986). As MOs are forming (many believe from the Golgi complex), a fibrous body becomes associated with each one (Ward and Klass, 1982; Wolf et al., 1978; reviewed in

L'Hernault, 2009). The fibrous body is composed of major sperm protein (MSP) filaments in polymerized bundles that are hexagonally packed (Ward and Klass, 1982; Wolf et al., 1978; reviewed in L'Hernault, 2009). FB-MO complexes are formed when a double membrane derived from the MO surrounds each FB. FB-MO complexes continue to enlarge during spermatogenesis, and reach their maximum size in secondary spermatocytes (Ward and Klass, 1982; reviewed in L'Hernault, 2009). During cytokinesis of meiosis II, FB-MO complexes localize to where astral microtubules are usually located, between the plasma membrane and the haploid nuclei, resulting in their asymmetrical division into the spermatids and not into the residual body (Wolf et al., 1978; reviewed in L'Hernault, 2009).

FB-MO complexes have three major parts: a head, a collar, and a body. The head is a membranous vesicle that is separated from the fibrous body by the collar; the collar is a narrow, "doughnut-shaped" constricted region. The cytoplasm within the FB-MO complex is shared between the head and the body (Wolf et al., 1978; Klass and Hirsh, 1981; Nishimura and L'Hernault, 2010). The fibrous body contains polymerized major sperm protein filaments surrounded by a double membrane (Ward and Klass, 1982; Wolf et al., 1978; reviewed in L'Hernault, 2009).

As secondary spermatocytes differentiate into spermatids, the double membrane surrounding the FB begins to retract, and the MSP filaments inside the FB begin to depolymerize into dimers (see Fig. 1) (Klass and Hirsh, 1981; King et al., 1992; Smith and Ward, 1998; reviewed in L'Hernault, 2009). The depolymerized MSP dimers spread throughout the cytoplasm of what is now the spermatid, and MO structures are no longer associated with MSP filaments (Ward and Klass, 1982; reviewed in Nishimura and L'Hernault, 2010). After the release of the depolymerized MSP dimers, the head of the MOs moves towards the plasma

membrane of the spermatids (Wolf et al., 1978; reviewed in Nishimura and L'Hernault, 2010). Eventually, during spermiogenesis, the head of the MO will permanently fuse with the plasma membrane of what was previously the spermatid, and deposit its contents (transmembrane proteins and glycoproteins) (Wolf et al., 1978; Xu and Sternberg, 2003; Chatterjee et al., 2005; Roberts and Ward, 1982; reviewed in L'Hernault, 2009).

Recent studies on MOs have demonstrated that they develop an internal acidity during spermatogenesis using a vacuolar H+-ATPase (V-ATPase), which couples the pumping of protons across plasma membranes with ATP hydrolysis (Gleason et al., 2012; reviewed in Paroutis et al., 2004). In spermatids, MOs are internally acidified using V-ATPase activity when they bud from the residual body (Gleason et al., 2012). V-ATPase activity is also known to be involved with the extension of the pseudopod during spermatid activation, and therefore the MO acidification could potentially be related to spermiogenesis (Gleason et al., 2012).

6. SPERMIOGENESIS

As previously defined, spermatogenesis is the process of activating spermatids into motile and fully functional gametes. Overall the process lasts approximately 10 minutes. However, the process rapidly changes the morphology of the sperm, converting them from spherical spermatids to asymmetrical spermatozoa. The major events of spermiogenesis include fusion of the MO heads with the spermatid plasma membrane, formation of the pseudopod that provides motility, and the initiation of motility (Klass et al., 1976; Nelson and Ward, 1980; Ward et al., 1981). Motility of the pseudopod is provided by controlled polymerization of the major sperm protein, as is the case in other nematode sperm (Ward and Klass, 1982; reviewed in Smith, 2006).

The exact activators that trigger spermatids to undergo spermiogenesis are not completely identified in either male or hermaphrodite *C. elegans*. Currently, it is believed that proteolysis is a likely trigger of spermatid activation, at least in *C. elegans* males (Standfield and Villeneuve, 2006). Additionally, other proteases, chloride channel inhibitors, and chemicals that elevate intracellular pH have been used as *in vitro* triggers of spermatid activation. However, none of these activators have been actually identified during *in vivo* spermiogenesis (Stanfield and Villeneuve, 2006; Ward et al., 1983; Machaca et al., 1996; Nelson and Ward, 1980). Male-derived spermatids are activated by components of the seminal fluid and are not activated until they are transferred into the hermaphrodite via copulation (Ward and Carrel, 1979). Hermaphrodite-derived spermatids, on the other hand, are activated shortly after production when they are physically pushed into the spermatheca by the first ovulated oocyte (Ward and Carrel, 1979; Stanfield and Villeneuve, 2006). Aside from the identity of the exact activators, spermatids that begin spermiogenesis are observed having long, thin extended spikes projecting outward (Nelson and Ward, 1980). These spikes thicken through the process of spermiogenesis, and often combine with each other (Shakes and Ward, 1989a). These spike projections and their adjacent cells give rise to the pseudopods (Shakes and Ward, 1989a; Nelson and Ward, 1980). A network of MSP polymers forms within the pseudopod at its front edge, while parts of the MSP network are disassembled at the pseudopod's rear, providing the now spermatozoa with the ability to crawl (Pavalko et al., 1988; Italiano et al., 2001). The MO fusion to the plasma membrane during spermiogenesis releases contents of the MO extracellularly, inserts transmembrane proteins permanently into the plasma membrane, and creates a permanent fusion pore (Wolf et al., 1978; Xu and Sternberg, 2003; Chatterjee et al., 2005; Roberts and Ward, 1982; reviewed in Nishimura and L'Hernault, 2010).

7. FERTILIZATION

In hermaphrodites, fertilization occurs in the spermatheca. Contractions of the oviduct wall force the mature oocyte into the spermatheca, which subsequently stretches to accommodate the oocyte. The presence of the first oocyte in the spermatheca triggers the opening of the spermathecal lumen, and the release of sperm from the spermatheca wall (Ward and Carrel, 1979). A single sperm will contact and fuse with each ovulated oocyte, creating a zygote that will eventually be expelled to the exterior through the vulva (Ward and Carrel, 1979; Hirsh et al., 1976; reviewed in Nishimura and L'Hernault, 2010). The pseudopod of the spermatozoa is possibly responsible for making first contact with the oocyte during fertilization (reviewed in Nishimura and L'Hernault, 2010). When the fertilized oocyte moves from the spermatheca into the uterus, it expels a number of sperm into the uterus with it. These sperm can be observed crawling back through the spermatheca-uterus valve into the spermatheca so that they are present for the next ovulation of a mature oocyte (Ward and Carrel, 1979).

Previous studies have reported that hermaphrodites produce about 370 sperm on their own. Nearly all hermaphrodite-derived sperm fertilize oocytes, but ovulation continues for a brief period after the sperm supply is exhausted. This results in unfertilized eggs being laid after fertilized embryos (Ward and Carrel, 1979; LaMunyon and Ward, 1995). Hermaphrodites produce 267 ± 67 progeny via self-fertilization when raised at 20°C (Ward and Carrel, 1979).

Interestingly, hermaphrodites that have been mated with males, as opposed to procreating via self-fertilization, will switch from using self-sperm to male-derived sperm for fertilization. This demonstrates that male sperm are stronger competitors for fertilizing oocytes than hermaphrodite sperm. As previously explained, male sperm are approximately 50% larger than hermaphrodite sperm. Additionally, male sperm appear to have a superior crawling velocity

compared to hermaphrodite sperm. Despite these correlations, the precise reason that male-derived sperm are superior to hermaphrodite-derived sperm for fertilization has not been conclusively established (LaMunyon and Ward, 1998; Ward and Carrel, 1979; reviewed in Nishimura and L'Hernault, 2010).

Hermaphrodite oocytes are fertilized with male sperm by copulation between the two sexes. During copulation, the copulatory bursa of the male is used to contact the hermaphrodite vulva. Upon contact between the male bursa and the hermaphrodite vulva, the male inserts its spicules into the vulva and ejaculates the hermaphrodite vulva into the uterus (Ward and Carrel, 1979). The number of sperm deposited into the hermaphrodite varies per copulation, and male-derived sperm have also been observed to spill out of the hermaphrodite when the male removes its spicules after copulation (Ward and Carrel, 1979). Male-derived sperm that are successfully deposited in the hermaphrodite uterus crawl towards and localize within the spermatheca. Once a hermaphrodite has been successfully inseminated with male-derived sperm, all of that hermaphrodites future progeny result from cross-fertilization. Additionally, it appears as though every male sperm capable of reaching the spermatheca eventually fertilizes an egg (Ward and Carrel, 1979).

8. PROJECT OVERVIEW AND GENOTYPES OF INTEREST

This study will investigate the numbers and distribution of MOs present in wild-type and a number of *spe* (spermatogenesis-defective) and *fer* (fertilization-defective) mutant genotypes. This research is an initial survey of MO counts per spermatid, something that has not been previously attempted. It is of particular interest because MOs are known to be morphologically abnormal within certain *spe* mutants (Gleason et al., 2006), and it is therefore plausible that an

additional source of phenotypic variation is the number of MOs found in spermatids. In this work, I am investigating the hypothesis that *C. elegans* spermatids may have the capacity to "count" MOs, or possess a specific number of MOs within spermatids based on sex and/or genotype.

The precise denotations of *spe* and *fer* are not limited to just spermatogenesis-defective or fertilization defective genotypes. More broadly, these mutants include genotypes that have irregular or abnormal sperm during spermatogenesis, spermiogenesis, and/or fertilization. The atypical nature of these mutants' sperm and related sperm functions causes mutant hermaphrodites of these genotypes to be self-sterile, meaning that they lay unfertilized oocytes as opposed to developing embryos. The presence of fully developed, unfertilized oocytes demonstrates that the *spe* and/or *fer* mutants do not affect oogenesis, but rather are causing sperm-based sterility (L'Hernault et al., 1988; McCarter et al., 1999). In order for *spe* and/or *fer* mutant hermaphrodites that are self-sterile to become fertile again, male-derived wild-type sperm must be used for fertilization (Argon and Ward, 1980; L'Hernault et al., 1988). Approximately 60 *spe* genes have been discovered using chemical mutagen treatments of hermaphrodites (L'Hernault, 1997; L'Hernault and Singson, 2000).

In this research, the genotypes examined were *spe-8(hc53)*, *spe-10(ok1149)V*; *him-8(e1489)IV*, *spe-21(hc113)III*; *him-5(e1490)V*, *spe-42(tm2421)V*; *him-8(e1489)IV*, *fer-14(ok2070)I*; *him-5(e1490)V*, and *peel-1(qq99)I; him-5(e1490)V*. Additionally, N2, *him-5(e1490)V*, *him-8(e1489)IV*, and *fem-3(q23)IV* genotypes were used as controls. Basic background on each of these genotypes will be explained below (see Table 1 for summary). Mutant genotypes were chosen so that there would be a large range of known spermatogenesis-

defective and fertilization-defective phenotypes for analysis. Phenotypic variety was considered because this type of quantitative MO survey has not been done before.

spe-8: *spe-8* is located on chromosome I (L'Hernault et al., 1988). The majority of *spe-8* mutants produce self-sterile hermaphrodites. However, *spe-8* mutants of the *hc134*ts allele have been observed to display hermaphrodite self-fertility at 16°C (L'Hernault et al., 1988). The following *spe-8* mutants have indistinguishable phenotypes: *hc40, hc50, hc53 hc79, hc85,* and *hc108,* (L'Hernault et al., 1988). This research was conducted using the *spe-8(hc53)I* mutant. The sterility of *spe-8* hermaphrodites results from the inability of *spe-8* spermatids to complete spermiogenesis and develop into motile spermatozoa. Within hermaphrodites, ovulation of the first oocyte pushes all the nonmotile spermatids (as opposed to spermatozoa in wild-type) into the uterus. Since they lack a pseudopod, these spermatids do not crawl back into the spermatheca. Interestingly, *spe-8* males produce functional spermatozoa and demonstrate fertility with hermaphrodites of the same or different genotypes (L'Hernault et al., 1988). *spe-8* hermaphrodite and male-derived spermatids have been found to activate successfully with *in vitro* treatment of triethanolamine, a known spermatid *in vitro* activator. Unlike wild-type, treatment of *spe-8* mutant spermatids with Pronase causes them extends spikes that do not resolve into a pseudopod (Shakes and Ward, 1989a). Additionally, as previously stated, *spe-8* mutant hermaphrodite-derived spermatids are able to activate into spermatozoa after exposure to male-derived seminal fluid, which contains the *in vivo* spermatid activators (Shakes and Ward, 1989a). These observations demonstrate that *spe-8* mutations are likely not sex-specific, and that *spe-8* mutations likely cause an arrest in hermaphrodite spermatid development that hinders spermiogenesis (Shakes and Ward, 1989a). *spe-8* is on chromosome I and encodes a non-receptor tyrosine kinase with a predicted SH2 domain (L'Hernault et al., 1988; Muhlrad and

Ward; unpublished data). I studied *spe-8* as an example of a group of five mutants with nominally identical cytological phenotypes: *spe-8, spe-12, spe-19, spe-27* and *spe-29* (reviewed in Nishimura and L'Hernault, 2010).

***spe-10*:** In *spe-10* mutants, spermatids have previously been observed to be about 60% the size of wild-type, and have off-centered nuclei (reviewed in Nishimura and L'Hernault, 2010). Additionally, the pseudopods of *spe-10* spermatozoa are shorter than those of wild-type, and are unable to give *spe-10* spermatozoa the crawling motility seen in wild-type (Shakes and Ward, 1989b). The *spe-10* FB-MOs disassemble and break down before spermatids bud from the residual body. During disassembly of *spe-10* FB-MOs, the FBs and the MOs separate from each other, resulting in abnormal segregation of both structures during spermatogenesis. The MOs disperse into spermatids that are budding from the residual body, but they have an irregular, vacuolated appearance. These MOs fail to fuse with the plasma membrane (Gleason et al., 2006; Shakes and Ward, 1989b). The FBs fail to move into budding spermatids, and are therefore left within the residual body. There have been instances where the FBs remaining in the residual body have been observed budding from the residual body as FB cytoplasts (Shakes and Ward, 1989b). *spe-10* is on chromosome V, and encodes a DHHC-CRD (cysteine-rich domain) zinc-finger transmembrane protein specifically found in sperm (Gleason et al., 2006). DHHC-CRD domain proteins are typically transmembrane proteins of eukaryotes, and have previously been studied for their role in the catalysis of protein palmitoylation (reviewed by Smotrys and Linder, 2004). *spe-10* has therefore been predicted to have a potential role in palmitoylation of one or more proteins required for proper regulation of FBs and MOs during spermatogenesis (Gleason et al., 2006). This research was completed using a *spe-10(ok1149)V*; *him-8(e1489)IV* strain. *spe-*

10(ok1149)V is a deletion mutant that lacks the majority of the *spe-10* gene and is likely null for SPE-10 function (Gleason et al., 2006).

***spe-21*:** Like *spe-10*, *spe-21* mutants produce nonfunctional spermatozoa. *spe-21* also encodes a transmembrane protein with a zinc finger motif and a cysteine-rich domain (Lindsey, 2002). Like *spe-10*, *spe-21* encodes a DHHC-CRD ring finger motif, however these two mutants have different phenotypes (Lindsey, 2002). Interestingly, *spe-10* and *spe-21* together represent a novel case of two genes for DHHC-CRD ring finger motifs that affect the same cellular pathway (Lindsey, 2002). Research on *spe-21* is currently being pursued. For my research, *spe-21(hc113)III*; *him-5(e1490)V* mutants were used.

***spe-42*:** *spe-42* mutants, belonging to the *spe-9* class of mutants (*spe-9, spe-13, spe-36, spe-38, spe-41, spe-42, fer-14* and *CeIzumo*), are fertilization defective, and produce hermaphrodites that are self-sterile (Kroft et al., 2005). Like other members of the *spe-9* mutant class, *spe-42* spermatozoa appear phenotypically normal, but fail to fertilize oocytes upon contact (Kroft et al., 2005; Singson et al., 1998). *spe-42* mutant male sperm also appears morphologically normal, and behaves as wild-type during crawling and sperm competition (Kroft et al., 2005). In general, *spe-9* class mutants are associated with defective sperm-oocyte interactions, either due to low binding affinity for sperm proteins and oocyte plasma membrane proteins, or normal sperm-oocyte binding, but defective sperm-oocyte fusion (reviewed in Nishimura and L'Hernault, 2010). *spe-42* is on chromosome V, and encodes a 6-pass transmembrane protein. SPE-42 has two functional domains, the first being a dendritic cell-specific transmembrane protein (DC STAMP) domain, and the second being a C4C4-type RING finger domain (Kroft et al., 2005; reviewed in Nishimura and L'Hernault, 2010). SPE-42 homologs have been observed in other metazoan species. The abundance of SPE-42 homologs

suggests that its functionality is conserved across species and that it is of great importance during fertilization (Kroft et al., 2005). DC-STAMP domains are involved with cell-cell fusion of osteoclasts in mammals (Miyamoto, 2006). More specifically, the *sneaky* gene, considered to be the homolog of *spe-42* in *Drosophila*, has been associated with the degradation of the sperm plasma membrane after it has entered an oocyte (Wilson et al., 2006). SPE-42 in *C. elegans* is thereby considered to potentially be involved with sperm-oocyte fusion through its DC-STAMP domain (Kroft et al., 2005). C4C4-type RING finger domains are known for their general involvement in protein-protein interactions (Borden et al., 2000). In humans, the related CNOT4-type RING finger protein has ubiquitin E3 ligase activity (Hanzawa et al., 2001; Albert et al., 2002). Therefore, SPE-42 likely associates with multiple sperm proteins, and/or that SPE-42 functions as a catalyst for ubiquitination of sperm proteins during fertilization (reviewed in Nishimura and L'Hernault, 2010). This research was completed using *spe-42(tm2421)V*; *him-8(e1489)IV* mutants.

***fer-14*:** *fer-14* fulfills all requirements to be placed into the *spe-9* mutant class (reviewed in Nishimura and L'Hernault, 2010). Unpublished results demonstrate that *fer-14* encodes a single-pass transmembrane protein, and that it appears to be nematode-specific (Kroft, Gleason, L'Hernault; unpublished). *fer-14* spermatozoa are morphologically identical to wild-type spermatozoa (Roberts and Ward, 1982). *fer-14* mutants are unable to fertilize upon spermatozoa-oocyte contact (L'Hernault, 1997). Additionally, male-derived *fer-14* spermatozoa are able to displace hermaphrodite spermatozoa, and render the contacted hermaphrodite self-sterile from the time of contact forward (Singson et al., 1999). This research was conducted using *fer-14(ok2070)I*; *him-5(e1490)V* mutants.

***peel-1*:** PEEL-1(*paternal effect epistatic embryonic lethal-1*) is expressed specifically in sperm, and encodes a toxin that is closely associated with an embryo-expressed antidote, *zeel-1*(*zygotic epistatic embryonic lethal-1*) (Seidel et al., 2008). The *zeel-1*/*peel-1* relationship has an incompatibility factor, where sperm expressing *peel-1* cause embryonic lethality in zygotes that are homozygous for a naturally occurring deletion of *zeel-1* (Seidel et al., 2008). It is therefore thought that ZEEL-1 has some type of antidote like capabilities in the oocyte when it encounters the otherwise toxic, sperm-delivered PEEL-1 (Seidel et al., 2008). *peel-1* encodes a newly discovered four-pass transmembrane protein. Little is otherwise known about the structure and specific function of PEEL-1 (Seidel et al., 2011). *peel-1* transcripts have been discovered in spermatocytes, but not in mature sperm, suggesting that *peel-1* toxicity is a consequence of delivery of the PEEL-1 protein by the sperm during fertilization (Seidel et al., 2011). *peel-1* transcripts have been discovered in spermatocytes, but not in mature sperm. This suggests that it is the PEEL-1 proteins, not the *peel-1* transcripts, which have toxic effects within zygotes (Seidel et al., 2011). Additionally, PEEL-1::GFP integrated transgene shows that PEEL-1 localizes within the FB-MO complexes of developing sperm (Seidel et al., 2011). PEEL-1::GFP localization staining is therefore a useful technique for studying MOs (Seidel et al., 2011). This research was conducted using *peel-1(qq99)I; him-5(e1490)V* mutants.

***him-5* & *him-8*:** *him* (*h*igh *i*ncidence of *m*ales) mutants are useful for conducting research requiring many males because males occur infrequently during hermaphrodite self-fertilization (Ward and Carrel, 1979; Hodgkin and Doniach, 1997). *him* mutants increase the incidence of males by increasing non-disjunction of the X chromosome during oogenesis (Hodgkin et al., 1979). For these *him* mutants, an abnormally high percentage of their oocytes will be nullo-X, meaning that they will develop into males upon self-fertilization (Hodgkin et al., 1979). *him-5*

mutants in particular have been noted to produce nullo-X oocytes at a rate of ~33% (Hodgkin et al., 1979). *him-5* and *him-8* mutants are used in this research because they have previously been shown to cause no additionally abnormalities in the anatomy of behavior of both males and hermaphrodites (Hodgkin et al., 1979). Previous work has shown that *him-8(e1489)V* mutants have self-progeny that is approximately 39% male (Phillips et al., 2005). In this research, many of the mutant strains examined were *him-5* or *him-8* along with their *spe* or *fer* genotype. This was done to increase males and thereby increase the amount of sperm available for observation. *him-5(e1490)V* and *him-8(e1489)III* mutants were therefore also used in this study as controls.

***fem-3(q23gf)*:** In wild-type hermaphrodites, *fem-3* is required for spermatogenesis, and its expression is highly regulated so that hermaphrodites are able to switch gamete production from sperm to oocytes (Barton et al., 1987). In wild-type males, *fem-3* is involved in soma and germ line development (Barton et al., 1987). The *fem-3(q23gf)IV* mutant has a temperature sensitive gain of function mutation that causes hermaphrodites grown at 25°C to produce exclusively spermatids and no oocytes, demonstrating that this mutation masculinizes the hermaphrodite germline (Barton et el., 1987). *fem-3(q23gf)IV* hermaphrodites are self-fertile at 15°C, but produce few to no progeny at 25°C (Barton et al., 1987). For the purposes of this research, *fem-3(q23gf)IV* hermaphrodites were used to analyze hermaphrodite sperm qualities because hermaphrodites normally convert all of their spermatids in spermatozoa but this does not occur in this mutant (Barton et al., 1987).

Because of the acidic nature of MOs present in maturing spermatids during spermatogenesis, MOs can be stained and counted using LysoSensor™Blue DND-192 (Gleason et al., 2012; reviewed in L'Hernault, 2009; reviewed in Nishimura and L'Hernault, 2010). Previously completed researching using this LysoSensor™Blue DND-192 technique has

documented that spermatids display blue dots characteristic of the expected size and position for MOs, and that these dots are no longer visible upon the conversion of spermatids to spermatozoa. This is an expected result because MOs are known to fuse with the plasma membrane during spermiogenesis, so they probably dump their formerly enclosed protons into the extracellular space (Gleason et al., 2012; reviewed in L'Hernault, 2009; reviewed in Nishimura and L'Hernault, 2010). By applying the technique of LysoSensor™Blue DND-192 staining of MOs in spermatids, here we quantitatively investigated the number of MOs present in the spermatids of wild-type and various *spe* mutants (see Table 1). Lastly, the number of MOs present in a spermatid was compared to the volume of that spermatid. This quantitative analysis gives insight into the effects of the aforementioned mutant genotypes on MOs, and potential expanded knowledge about the role of MOs during spermatogenesis and spermiogenesis.

Table 1: Summary of the Major Phenotypic Characteristics for the Genotypes of Interest

Mutant Genotype	Major Phenotypic Characteristics	References
spe-8(hc53)I	Hermaphrodites: self-sterile, spermiogenesis defective Males: produce normally functioning sperm	L'Hernault et al., 1988.
spe-10(ok1149)V; him-8(e1489)IV	Males & Hermaphrodites: small spermatids, short pseudopods, premature disassembly of FB-MOs, vacuolated MOs in spermatids, FBs remain in residual body	Gleason et al., 2006; Shakes and Ward, 1989b
spe-21(hc113)III; him-5(e1490)V	Males & Hermaphrodites: Nonfunctional spermatozoa; currently under investigation	W. C. Lindsey, Ph.D. thesis, unpublished results.
spe-42(tm2421)V; him-8(e1489)IV	Hermaphrodites: Self-sterile, *spe-9* class, morphologically normal oocytes and spermatozoa, failure to fertilize upon gamete contact Males: produce morphologically normal spermatozoa, behave normally during competition and crawling, fail to fertilize oocytes	Kroft et al., 2005; Singson et al., 1998.
fer-14(ok2070)I; him-5(e1490)V	Hermaphrodites: self-sterile, *spe-9* class, failure to fertilize upon gamete contact Males: spermatozoa are able to crawl and compete normally, fail to fertilize oocytes	Kroft, Gleason, L'Hernault; unpublished; L'Hernault, 1997; Roberts and Ward, 1982; Singson et al., 1999.
peel-1(qq99)I; him-5(e1490)V	Males: encodes a sperm-derived toxin located in the FB-MO complexes during spermatogenesis, causes embryo lethality when sperm contains PEEL-1 and zygote fails to express ZEEL-1	Seidel et al., 2008; Seidel et al., 2011.

Table 1: Summary of the Major Phenotypic Characteristics for the Genotypes of Interest		
Mutant Genotype	**Major Phenotypic Characteristics**	**References**
him-5(e1490)V	Hermaphrodites: increase nondisjunction of X chromosome during oogenesis, causes an increased abundance of males in self-progeny	Hodgkin et al., 1979.
him-8(e1489)III	Hermaphrodites: increase nondisjunction of X chromosome during oogenesis, causes an increased abundance of males in self-progeny	Hodgkin et al., 1979.
*fem-3(q23gf)IV**	Hermaphrodites: produce an excess of spermatids, fail to produce oocytes, masculinization of hermaphrodite germline	Barton et al., 1987.

* *fem-3(q23gf)IV* was grown at 25°C. All other strains were grown at 20°C.

9. MATERIALS AND METHODS

Strains, Culture, and Nomenclature:

Standard *C. elegans* nomenclature and techniques were used during this research (Horvitz et al., 1979). N2 wild-type *C. elegans* of the Bristol variety was used as the control strain for these experiments. The following mutant strains were used: *him-8(e1489)IV* (Hodgkin et al., 1979), *him-5(e1490)V* (Hodgkin et al., 1979), *fem-3(q23gf)IV* (Barton et al., 1987), *spe-10(ok1149)V*; *him-8(e1489)IV* (Shakes and Ward, 1989b), *spe-8(hc53)I* (L'Hernault et al., 1988), *spe-21(hc113)III*; *him-5(e1490)V* (Lindsey, 2002), *spe-42(tm2421)V*; *him-8(e1489)IV* (Kroft et al., 2005), *fer-14(ok2070)I*; *him-5(e1490)V* (T. L. Kroft, E. J. Gleason and S. W. L'Hernault, unpublished), and *peel-1(qq99)I*; *him-5(e1490)V* (Seidel et al., 2008).

All strains were cultured and manipulated as previously described (Brenner, 1974). Strains were cultured on NGM agar 6 cm plates each containing three droplets of OP50. All cultures used for staining were incubated at 20°C, with the exception of the *fem-3(q23gf)IV* strain which was incubated at 25°C for experiments but maintained at 20°C. To maintain culture propagation, small chunks were excised and placed onto fresh NG agar plates along with 3 OP50 droplets approximately every two weeks. I completed all MO counts and spermatid measurements during 2013.

Collection and Isolation of Males:

Males were isolated on 6 cm spotted NGM agar plates for a period of 36-48 hours before dissection. Plates with isolated males contained no other hermaphrodites and/or eggs.

Dissection and Staining:

Worms were dissected in 2-4 µl of dissection buffer, which was 1X sperm medium (SM) [50 mM HEPES (pH 7.8), 25 mM KCl, 45 mM NaCl, 1 mM $MgSO_4$, 5 mM $CaCl_2$] that has been modified by the addition of 10 mM dextrose [SM (pH 7.8)/dextrose] (Machaca et al., 1996). LysoSensor™ Blue DND-192 was used to stain the MOs within the spermatids (Gleason et al., 2012). Stocks of LysoSensor™ Blue DND-192 from Molecular Probes® (Eugene, OR) were supplied as 1 mM in dimethyl sulfoxide. The LysoSensor™ Blue DND-192 stain was diluted into the dissection buffer to a working concentration of 1-10 µM. Dissection buffer containing LysoSensor™ Blue DND-192 was shielded from light during the dissection process (Gleason et al., 2012).

Just before dissection, single worms were placed in 2-4 µl of the previously described dissection buffer on individual wells of 8-well multi-test glass slides from (MP Biomedicals, LLC, Santa Ana, CA). Worms were then sliced through the gonad using 27-gauge hypodermic needles. Glass slides containing dissected worms were placed in a humid chamber for 10 minutes at 25°C before cover slips were applied.

Image Collection and MO Counting:

The LysoSensor™ Blue DND-192 stained MOs within spermatids were viewed using an Olympus BX60 with a 1.35 numerical aperture 100X oil-immersion objective lens. Epi-fluorescence of stained MOs was imaged using a DAPI filter pack and captured with a SensiCam digital camera (Cooke, Auburn Hills, MI) controlled by SlideBook software (Intelligent Imaging

Innovations, Denver, CO). SlideBook software was used to collect Z-axis stacks of 11-30, and 12-bit images were captured every .44-.88 μm. The majority of images within the Z-stacks were collected approximately every 0.65 μm. A nearest-neighbor deconvolution algorithm within the SlideBook software was applied to the images. Images were then converted to Z-axis projections, again using capabilities of the SlideBook software. The diameters of individual spermatids were measured within SlideBook using the software's ruler function over images captured with a DIC filter. The manipulated images were exported from SlideBook as 16-bit tif images. The 16-bit tif images exported from SlideBook were re-opened in ImageJ software (NIH, Bethesda, MD). The cell counter plugin within ImageJ was used to assist in counting MOs. The images included at the end of this paper were compiled using PhotoShop CS3 (Adobe Systems, San Jose, CA).

10. RESULTS

Table 2 provides a summary of the major results in this research. Raw data for all spermatids analyzed is available in Appendix 1. Figures 2, 3, and 4 below show LysoSensor™ Blue DND-192 stained MOs for the stated genotypes. N2 male-derived spermatids were found to have about 45% more volume than *him-5* male-derived spermatids, about 200% more volume than N2 hermaphrodite-derived spermatids, about 200% more volume than *him-5* hermaphrodite-derived spermatids, and about 85% larger than *fem-3* hermaphrodite-derived spermatids. N2 male-derived spermatids also had about 55% more MOs than *him-5* male-derived spermatids, and about 130% more MOs than N2 hermaphrodite-derived spermatids. *him-5* male-derived spermatids were found to have 110% more volume than those N2 hermaphrodite-derived spermatids, about 110% more volume than those of *him-5* hermaphrodite-derived spermatids, and about 38% less volume than those of *him-8* male-derived

spermatids. *him-5* male-derived spermatids also had about 16% fewer MOs than N2 male-derived spermatids, about 25% fewer MOs than *him-8* male-derived spermatids, about 100% more MOs than N2 hermaphrodite-derived spermatids, and about 33% more MOs than *him-5* hermaphrodite-derived spermatids. *him-8* male-derived spermatids had about 190% more volume than N2 hermaphrodite-derived spermatids, about 200% more volume than *him-5(e1490)*V hermaphrodite-derived spermatids, and about 80% more volume than *fem-3*hermaphrodite-derived spermatids. *him-8* male-derived spermatids had about 150% more MOs than N2 hermaphrodite-derived spermatids, about 66% more MOs than *him-5* hermaphrodites, and about 25% more MOs than *fem-3* hermaphrodite-derived spermatids. N2 hermaphrodite-derived spermatids had about the same volume as *him-5* hermaphrodite-derived spermatids, and about 40% less volume than *fem-3* hermaphrodite-derived spermatids. N2 hermaphrodite-derived spermatids also had 50% fewer MOs than *him-5* hermaphrodite-derived spermatids, and about 100% fewer MOs than *fem-3* hermaphrodite-derived spermatids. *him-5* hermaphrodite-derived spermatids had about 66% less volume than *fem-3* hermaphrodite-derived spermatids, and about 33% fewer MOs than *fem-3* hermaphrodite-derived spermatids. Overall for my control genotypes, N2 male-derived spermatids had the highest average volume, and *him-8* male-derived spermatids had the highest average number of MOs. N2 hermaphrodite-derived spermatids were found to have the fewest MOs of all control genotypes, and *him-5* hermaphrodite-derived spermatids and N2 hermaphrodite-derived spermatids tied for lowest average volume of all control genotypes.

spe-8 male mutants were maintained as mating plates and obtaining large numbers of males did not require a *him* mutation. Comparing *spe-8* male-derived spermatids to N2 male-derived spermatids, *spe-8* male-derived spermatids had about 20% less volume than N2 male-

derived spermatids, about 150% more volume than N2 hermaphrodite-derived spermatids, about 30% more MOs than N2 male-derived spermatids, and about 200% more MOs than N2 hermaphrodite-derived spermatids.

spe-10 male-derived spermatids had about 20% more volume than the related control *him-8* male-derived spermatids, but were found to have the same number of MOs as *him-8* male-derived spermatids. Compared to N2 spermatids, *spe-10* male-derived spermatids had 20% more volume than N2 males, and about 150% more volume than N2 hermaphrodites. *spe-10* male-derived spermatids also had about 30% more MOs than N2 males, and about 200% more MOs than N2 hermaphrodites.

spe-21; him-5 male-derived spermatids had about 30% less volume than the *him-5* male control, and about 60% more volume than the *him-5* hermaphrodite control. *spe-21; him-5* male-derived spermatids had about 33% fewer MOs than the *him-5* male control, and about the same number of MOs as the *him-5* hermaphrodite control.

spe-42; him-8 male-derived spermatids had about 45% less volume than the control *him-8* males. *spe-42; him-8* male-derived spermatids also had about 30% fewer MOs than the control *him-8* males.

fer-14; him-5 male-derived spermatids had about 40% more volume than the control *him-5* males, and about 200% more volume than the control *him-5* hermaphrodites. *fer-14; him-5* male-derived spermatids also had about 50% more MOs than the *him-5* males, and about 100% more MOs than the related *him-5* hermaphrodites.

peel-1; him-5 male-derived spermatids had about 40% more volume than *him-5* male-

derived spermatids, and about 200% more volume than *him-5* hermaphrodite-derived spermatids. *peel-1;him-5* male-derived spermatids also had about 60% more MOs than *him-5* male-derived spermatids, and about 110% more MOs than *him-5* hermaphrodite-derived spermatids.

Table 2: Results Summary

Genotype	Sex	Spermatid diameter (μm)	Spermatid volume (μm³)	# of MO's	# of MO's: Spermatid Volume (μm³)	*n* =
N2	herm	3.9 ± 0.1	33 ± 1.9	6 ± 0.4	0.2 ± 0.01	8
*fem-3(q23gf)*IV*	herm	4.6 ± 0.1	55 ± 3.1	12 ± 0.4	0.2 ± 0.01	46
*him-5(e1490)*V	herm	4.0 ± 0.1	33 ± 2.7	9 ± 0.5	0.3 ± 0.02	10
N2	male	5.6 ± 0.2	102 ± 7.1	14 ± 0.4	0.2 ± 0.02	40
*him-5(e1490)*V	male	5.1 ± 0.1	70 ± 2.6	12 ± 0.6	0.2 ± 0.01	30
*him-8(e1489)*III	male	5.6 ± 0.1	97 ± 4.4	15 ± 0.4	0.2 ± 0.01	52
*spe-8(hc53)*I	male	5.4 ± 0.03	84 ± 1.5	18 ± 0.2	0.2 ± 0.01	111
spe-10(*ok1149*)V; *him-8*(*e1489*)IV	male	6.1 ± 0.1	118 ± 3.2	15 ± 0.3	0.1 ± 0.004	60
spe-21(*hc113*)III; *him-5*(*e1490*)V	male	4.6 ± 0.1	53 ± 2.2	9 ± 0.3	0.2 ± 0.01	30
spe-42(*tm2421*)V; *him-8*(*e1489*)IV	male	4.6 ± 0.1	53 ± 2.9	11 ± 0.3	0.2 ± 0.01	52
fer-14(*ok2070*)I; *him-5*(*e1490*)V	male	5.7 ± 0.05	98 ± 2.5	18 ± 0.4	0.2 ± 0.004	42
*peel-1(qq99)*I	male	5.6 ± 0.1	97 ± 4.5	19 ± 0.5	0.2 ± 0.02	40

**fem-3(q23)* hermaphrodites were grown at 25°C. All other strains were grown at 20°C.

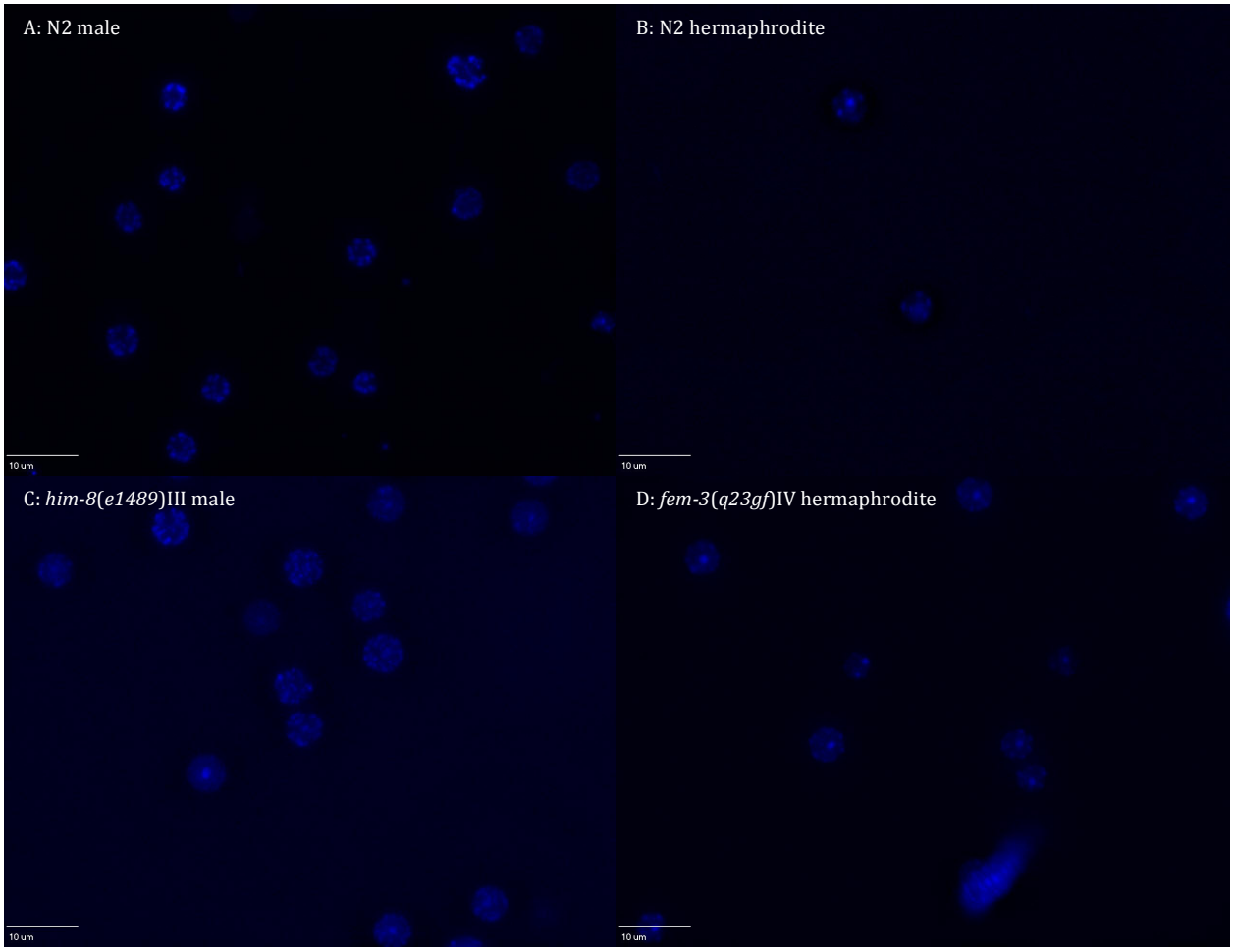

Fig. 2: (A) N2 male-derived spermatids, **(B)** N2 hermaphrodite-derived spermatids, **(C)** *him-8*(*e1489*)III, **(D)** *fem-3*(*q23gf*)IV hermaphrodite-derived spermatids with LysoSensor™Blue DND-192 stained MOs. N2 male-derived spermatids have visibly more MOs than N2 hermaphrodite-derived spermatids.

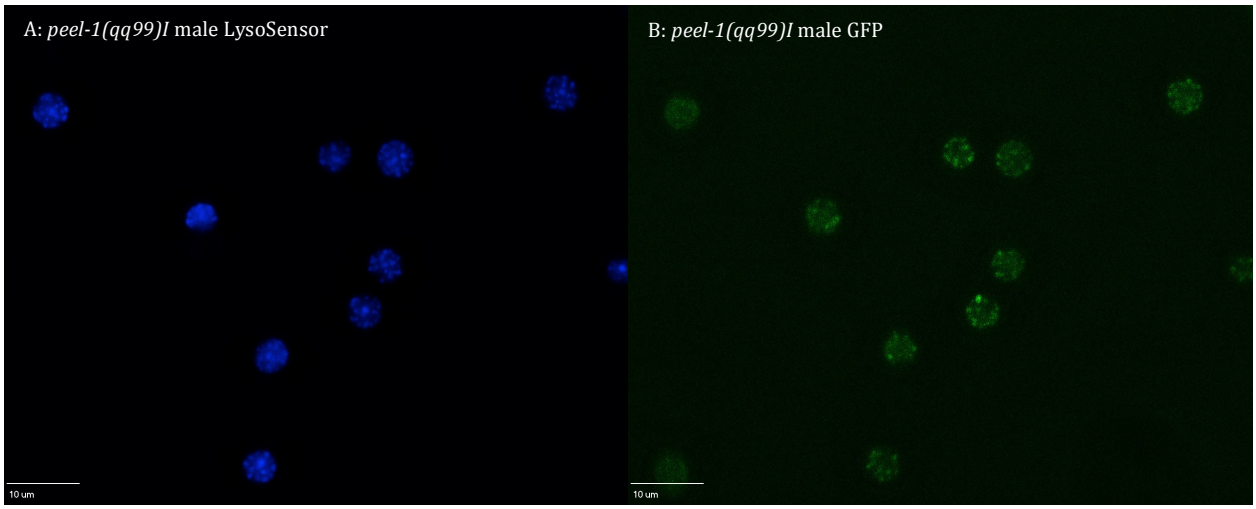

Fig. 3: (A) *peel-1(qq99)I; him-5(e1490)V* male-derived spermatids with LysoSensor™Blue DND-192 stained MOs. **(B)** *peel-1(qq99)I; him-5(e1490)V* male-derived spermatids with PEEL-1::GFP expression localized in the FB-MOs.

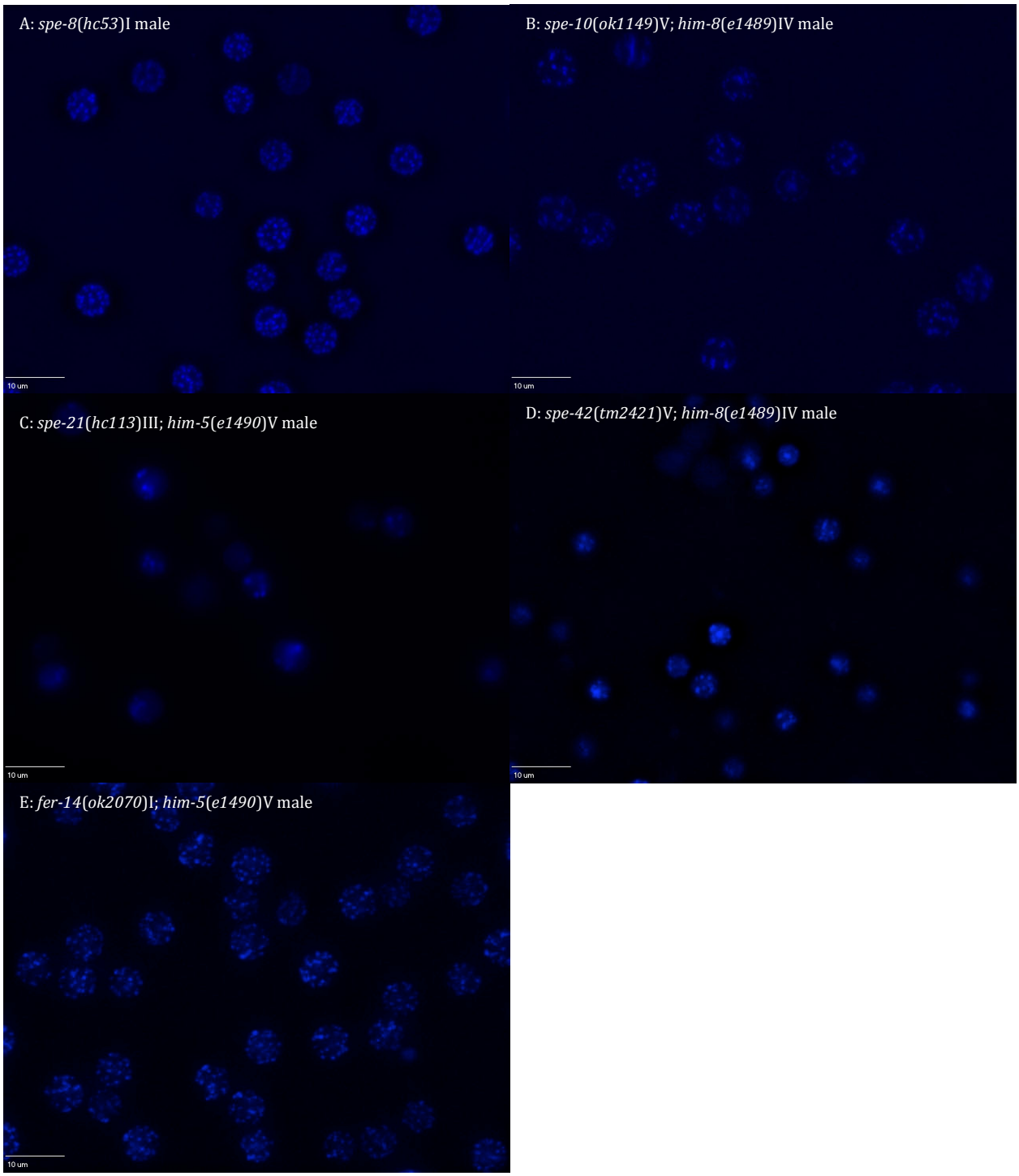

Fig. 4: (A) *spe-8*(*hc53*)I male-derived spermatids, **(B)** *spe-10*(*ok1149*)V; *him-8*(*e1489*)IV male-derived spermatids, **(C)** *spe-21*(*hc113*)III; *him-5*(*e1489*)IV male-derived spermatids, **(D)** *spe-42*(*tm2421*)V; *him-8*(*e1489*)IV male-derived spermatids, and **(E)** *fer-14*(*ok2070*)I; *him-5*(*e1490*)V male-derived spermatids with LysoSensor™Blue DND-192 stained MOs. *spe-8*(*hc53*)I, *spe-10*(*ok1149*)V; *him-8*(*e1489*)IV, and *fer-14*(*ok2070*)I; *him-5*(*e1490*)V male-derived spermatids have visibly more MOs than *spe-21*(*hc113*)III; *him-5*(*e1489*)IV or *spe-42*(*tm2421*)V; *him-8*(*e1489*)IV male-derived spermatids.

11. DISCUSSION AND CONCLUSIONS

This work quantitatively analyzed the number of MOs present in spermatids of various genotypes. MO counts were possible because of the acidic nature of the MOs present in developing spermatids, which could consequentially be stained using LysoSensor™Blue DND-192 treatment (Gleason et al., 2012; reviewed in L'Hernault, 2009; reviewed in Nishimura and L'Hernault, 2010).

As the standard error values (see Table 2) demonstrate, this work would benefit from increasing the number of spermatids that were analyzed. However, as these results currently stand, there are a number of potentially significant findings in this work. Firstly, these quantitative data for the control genotypes, *him-8*, *him-5*, *fem-3*, and N2 (Bristol var.), demonstrates that hermaphrodite-derived spermatids have narrower diameters and fewer MOs per spermatid than male-derived spermatids (see Table 2). Correspondingly, the average spermatid volume of all three hermaphrodite controls (*him-5*, *fem-3*, and N2) was found to be about ~40 μm^3, which is substantially lower than that of average of the male controls (*him-8*, *him-5*, and N2), which was about ~90 μm^3. Also, I found that males of my control genotypes had about 14 MOs per spermatid, whereas control hermaphrodites had ~9 MOs per spermatid. This difference indicates that hermaphrodite-derived spermatids of our controls had, on average, 55% fewer MOs per spermatid than our control males. The narrower diameters of hermaphrodite-derived spermatids in this work confirm a previous finding that hermaphrodite-derived sperm are significantly smaller than male-derived sperm (LaMunyon and Ward, 1995, 1998). A plausible explanation for the discrepancy in MO number per spermatid between males and hermaphrodites of our control genotypes is that there is a potential relationship between spermatid size and number of MOs, simply based on the available volume within each spermatid.

A second potential explanation is that an increased number of MOs in male-derived spermatids is advantageous for male-derived sperm during sperm competition. This hypothesis could offer insight into additional reasons as to why male-derived sperm are observed successfully outcompeting hermaphrodite sperm during fertilization (reviewed in L'Hernault, 2009; LaMunyon and Ward, 1995, 1998). From just analyzing the differences between male and hermaphrodite control genotypes in spermatid volume and MO number, it becomes plausible that *C. elegans* spermatids have some sort of capacity to "count" MOs, or allot only a certain number depending on sex and/or genotype into developing spermatids. While volumes varied widely, depending on genotype, the number of MOs per μm^3 was 0.2, or close to it. This novel idea requires significant further experimentation to confirm, but from the findings in this work, it does not seem far-fetched.

A second finding from this work is that *spe-8* male-derived spermatids had little variation from our control male-derived spermatids in volume or from our control male-derived spermatids number of MOs. *spe-8* hermaphrodite-derived spermatids fail to complete spermiogenesis and become functional spermatozoa, whereas *spe-8* male-derived spermatids are able to fertilize oocytes and activate normally (L'Hernault et al., 1988). As this work shows, *spe-8* male-derived spermatids are similar to wild-type in spermatid volume or number of MOs, which we would expect since *spe-8* male-derived spermatids undergo spermiogenesis and are capable or fertilization. Future analysis of *spe-8* hermaphrodites would be useful for further interpretation of these results.

The *spe-10* male-derived spermatids examined in this work call into doubt previous work that indicated that *spe-10* mutant spermatids are smaller than wild-type (reviewed in Nishimura and L'Hernault, 2010). This work interestingly found that *spe-10* male-derived spermatids had

the largest average volume of all genotypes examined. In comparing the data from *spe-10* male-derived spermatids to the control *him-8* male-derived spermatids, minimal differences were noted in spermatid diameter and counts of number of FB-MOs per spermatid. This result is surprising because *spe-10* mutants were specifically chosen for their affected FB-MO phenotype that causes FB-MO disassembly, failure of MOs to fuse with the plasma membrane, and failure of FBs to bud into developing spermatids (Gleason et al., 2006; Shakes and Ward, 1989b; L'Hernault and Arduengo, 1992). While it is known that *spe-10* mutants clearly have atypical FB-MOs in their spermatids, this work indicates that the cause is likely not quantitatively based on MOs. Also, as electron microscopy indicates, the *spe-10* mutant spermatids are known to have significantly abnormal FB-MO phenotype (Gleason et al., 2006; Shakes and Ward, 1989b; L'Hernault and Arduengo, 1992). This work demonstrates that many MOs within *spe-10* mutant male-derived spermatids are still able to be stained using LysoSensor™Blue DND-192 treatment. The actual staining of many MOs in *spe-10* mutant spermatids is a novel result itself because it indicates that the V-ATPase in *spe-10* mutant male-derived spermatids is still functioning and creating an acidic internal environment within the MOs (Gleason et al., 2012). As mentioned above, most strains had 0.2 MOs per μm^3. *spe-10* was the one mutant that deviated from 0.2 MOs per μm^3, so it is possible that not all of its MOs were stainable because of the above-discussed structural defects. Alternatively, perhaps the MO counting mechanism is defective in *spe-10* mutants.

spe-21 male-derived spermatids were found in this work to have a significantly lower number of MOs, and a significantly lower average volume than the related control *him-5* males. In fact, *spe-21* male-derived spermatids were found to have the lowest number of MOs than any other mutant genotype analyzed. This is an extremely interesting result. One possible

explanation is that some *spe-21* MOs do not stain with the vital dye that was used. While the specifics of the *spe-21* mutation and phenotype are still under investigation, this research suggests that the *spe-21* mutants' production of non-functional spermatozoa (Lindsey, 2002) could potentially be linked to its diminished number of MOs in its spermatids, and/or its lower average spermatid volume. More spermatids from this genotype would have to be analyzed to strengthen the statistical significance behind this proposal.

spe-42 male-derived spermatids had a lower number of MOs than both the related control *him-8*, and the overall average number of MOs for all control genotypes. Also, *spe-42* male-derived spermatids had about 45% less volume than the related control *him-8* males, and significantly less volume than the average of all control male genotypes. It was thought that *spe-42* mutants produce morphologically normal sperm that fail to fertilize oocytes upon contact (Kroft et al., 2005). This research suggests, though, that *spe-42(tm2421)V* spermatids are not morphologically normal, but in fact have less volume than wild-type, and fewer MOs per spermatid. More spermatids of this genotype (for both sexes) would need to be analyzed to improve the statistical confidence of this claim, but this preliminary research does permit the possibility that the failure of *spe-42* spermatozoa to fertilize oocytes (Kroft et al., 2005) could be related to a decreased spermatid volume and a diminished number of MOs.

The finding that *fer-14* male-derived spermatids analyzed in this work had more volume, and more MOs than the related *him-5* control males is interesting in comparison to the *spe-42* male spermatid results. Both of these mutant genotypes are part of the *spe-9* mutant class, and have previously been observed to be morphologically normal, but fail to fertilize oocytes on contact (Kroft et al., 2005; Roberts and Ward, 1982; L'Hernault, 1997; Kroft, Gleason, L'Hernault; unpublished; Singson et al., 1999). While *spe-42* male-derived spermatids had a

decreased volume and diminished number of MOs compared to the related *him-8* controls, *fer-14* male-derived spermatids had an increased volume and increased number of MOs compared to the *him-5* controls. While both mutants fail to fertilize oocytes upon contact (Kroft et al., 2005; L'Hernault, 1997), it is unclear from this work whether that phenotype has any direct correlation to spermatid volume and/or MO number.

peel-1;him-5 male-derived spermatids had more volume and more MOs per spermatid than *him-5* male-derived spermatids. Within this work, *peel-1* male-derived spermatids were included because the strain is known to have GFP expression within its FB-MO complexes. This work found these *peel-1* male-derived spermatids could also be stained with LysoSensor™Blue DND-192 to visualize MOs. This indicates that *peel-1* could be crossed into other mutants to allow MO counts based on GFP localization and assessment of acidification ability based on LysoSensor™Blue DND-192 staining. One potential source of error to consider within my thesis research is that using LysoSensor™Blue DND-192 staining to determine MO numbers would not work if mutant sperm have MOs that fail to acidify. Therefore, crossing *peel-1* into *spe* mutant genotypes of interest would provide an additional way to assess the number of MOs in spermatids that is not based on MO acidity.

Overall, this research represents a first attempt at a novel exploration of MO number per spermatid within the indicated mutant genotypes, and the related control genotypes. While there is room for improvement within the statistical significance of the data within this work, these initial values offer insight into how the number of MOs per spermatid is potentially related to various *spe* and *fer* genotypes. Future work should firm up what my work already indicates are significant differences in MO number per spermatid for various mutant genotypes, and extend this approach to other related *spe* genotypes in the future. The results here indicate that there are

potentially significant variations in the number of MOs in spermatids of different genotypes. This finding is of importance because it strengthens my hypothesis that *C. elegans* spermatids have the capacity to "count" MOs and that this somehow linked to spermatid volume. Additional quantitative analysis of MOs in hermaphrodite-derived spermatids, and how their number varies among *spe* mutants, would also prove useful.

REFERENCES

Albert, T.K., Hanzawa, H., Legtenberg, Y.I., de Ruwe, M.J., van den Heuvel, F.A., Collart, M.A., Boelens, R., Timmers, H.T. 2002. Identification of a ubiquitin-protein ligase subunit within the CCR4-NOT transcription repressor complex. EMBO J 21:355–364.

Altun ZF, Hall DH. 2006. *Atlas of C elegans Anatomy:* an illustrated handbook. "Hermaphrodite Anatomy." http://www.wormatlas.org/ver1/handbook/contents.htm.

Argon, Y., and Ward, S. 1980. *Caenorhabditis elegans* fertilization-defective mutants with abnormal sperm. Genetics 96:413-433.

Barr, M. M., and Garcia, L. R. 2006. Male mating behavior. In: WormBook, ed. The *C. elegans* Research Community, WormBook, doi/10.1895/wormbook. 1.78. 1.

Barton, M. K., Schedl, T. B., and Kimble, J. 1987. Gain-of-function mutations of *fem-3*, a sex-determination gene in *Caenorhabditis elegans*. Genetics 115:107-119.

Blelloch, R., and Kimble, J. 1999. Control of organ shape by a secreted metalloprotease in the nematode *Caenorhabditis elegans*. Nature 399:586-590.

Borden, K.L. 2000. RING domains: master builders of molecular scaffolds? J Mol Biol
295:1103–1112.

Brenner, S. 1974. The genetics of *Caenorhabditis elegans*. Genetics 77:71-94.

Byerly, L., Cassada, R. C., and Russell, R. L. 1976. The life cycle of the nematode *Caenorhabditis elegans*: I. wild-type growth and reproduction. Dev Biol 51:23-33.

Church, D. L., Guan, K. L., and Lambie, E. J. 1995. Three genes of the MAP kinase cascade, *mek-2*, *mpk-1/sur-1* and *let-60 ras*, are required for meiotic cell cycle progression in *Caenorhabditis elegans*. Development 121:2525-2535.

Chitwood, B.G. and Chitwood, M.B.H. 1974. *Introduction to Nematology*. Baltimore: University Park Press.

Crittenden, S. L., Troemel, E. R., Evans, T. C., and Kimble, J. 1994. GLP-1 is localized to the mitotic region of the *C. elegans* germ line. Dev 120:2901-2911.

Chatterjee, I., Richmond, A., Putiri, E., Shakes, D.C., and Singson, A. 2005. The *Caenorhabditis elegans spe-38* gene encodes a novel four-pass integral membrane protein required for sperm function at fertilization. Dev 132:2795–2808.

Ellis, R., and Schedl, T. 2007. Sex determination in the germ line. In: WormBook, ed. The C. elegans Research Community, WormBook, doi/10.1895/wormbook. 1.82. 2.

Emmons, S.W. and Sternberg, P.W. Male development and behavior. In: Riddle D., Blumentahl R., Meyer B.J., and Priess, J. editors. *C. elegans II*. Cold Spring Harbor, NY: Cold Spring Harbor Laboratory Press. 295-334.

Garcia, L. R., Mehta, P., and Sternberg, P. W. 2001. Regulation of distinct muscle behaviors controls the *C. elegans* male's copulatory spicules during mating. Cell 107:777-88.

Gleason, E. J., Hartley, P. D., Henderson, M., Hill-Harfe, K. L., Price, P. W., Weimer, R.M., and L'Hernault, S. W. 2012. Developmental genetics of secretory vesicle acidification during *Caenorhabditis elegans* spermatogenesis. Genetics 191:477-491.

Gleason E.J., Lindsey W.C., Kroft T.L., Singson A.W., L'Hernault S.W. 2006. *spe-10* encodes a DHHC-CRD zinc finger membrane protein required for endoplasmic reticulum/Golgi membrane morphogenesis during *Caenorhabditis elegans* spermatogenesis. Genetics 172:145–158.

Hall, D. H., Winfrey, V. P., Blaeuer, G., Hoffman, L. H., Furuta, T., Rose, K. L., and Greenstein, D. 1999. Ultrastructural Features of the Adult Hermaphrodite Gonad of *Caenorhabditis elegans*: Relations between the Germ Line and Soma. Dev Biol 212: 101-123.

Hansen, D., Wilson-Berry, L., Dang, T., and Schedl, T. 2004. Control of the proliferation versus meiotic development decision in the *C. elegans* germline through regulation of GLD-1 protein accumulation. Development 131:93-104.

Hanzawa, H., de Ruwe, M.J., Albert, T.K., van Der Vliet, P.C., Timmers, H.T., and Boelens R. 2001. The structure of the C4C4 ring finger of human NOT4 reveals features distinct from those of C3HC4 RING fingers. J Biol Chem 276:10185-10190.

Hirsh D., Oppenheim D., and Klass M. 1976. Development of the reproductive system of *Caenorhabditis elegans*. Dev Biol 49:200-219.

Hodgkin, J.A. 1974. Genetic and Anatomical Aspects of the *Caenorhabditis elegans* Male. University of Cambridge, thesis.

Hodgkin, J. and Doniach, T. 1997. Natural variation and copulatory plug formation in *Caenorhabditis elegans*. Genetics 146**:** 149-164.

Hodgkin, J., Horvitz, H. R., and Brenner, S. 1979. Nondisjunction mutants of the nematode *Caenorhabditis elegans*. Genetics 91:67-94.

Horvitz, H. R., Brenner, S., Hodgkin, J., and Herman, R. K. 1979. A uniform genetic nomenclature for the nematode *Caenorhabditis elegans*. Molecular and General Genetics 175:129-133.

Italiano J.E., Roberts T.M., Stewart M., and Fontana C.A. 1996. Reconstitution *in vitro* of the motile apparatus from the amoeboid sperm of *Ascaris* shows that filament assembly and bundling move membranes. Cell 84:105–114.

Italiano, J.E. Jr, Stewart, M., and Roberts, T.M. 2001. How the assembly dynamics of the nematode major sperm protein generate amoeboid cell motility. Int Rev Cytol 202:1-34.

Jaramillo-Lambert, A., Ellefson, M., Villeneuve, A.M., and Engebrecht, J., 2007. Differential timing of S phases, X chomosome replication, and meiotic prophase in the *C. elegans* germ line. Dev. Biol. 308:206–221.

Kelleher, J. F., Mandell, M. A., Moulder, G., Hill, K. L., L'Hernault, S. W., Barstead, R., and Titus, M. A. 2000. Myosin VI is required for asymmetric segregation of cellular components during *C. elegans* spermatogenesis. Current Biology 10:1489-1496.

Kimble, J., and Crittenden, S.L., 2007. Controls of germline stem cells, entry into meiosis, and the sperm/oocyte decision in *Caenorhabditis elegans*. Annu Rev Cell Dev Biol 23:405–433.

Kimble J, and Hirsh D. 1979. The Postembryonic cell lineages of the hermaphrodite and male gonads in *Caenorhabditis elegans*. Developmental Biology 70:396-417.

Kimble J., and Ward S. 1988. Germ-line development and fertilization. In: Wood WB, editor. The nematode *Caenorhabditis elegans*. Cold Spring Harbor, NY: Cold Spring Harbor Laboratory Press.191–213.

Kimble, J. E., and White, J. G. 1981. On the control of germ cell development in *Caenorhabditis elegans.* Dev Biol 81:208-219.

King, K.L., Stewart, M., Roberts, T.M., and Seavy, M. 1992. Structure and macromolecular assembly of two isoforms of the major sperm protein (MSP) from the amoeboid sperm of the nematode, *Ascaris suum*. J Cell Sci 101:847–857.

Klass, M. R., and Hirsh, D. 1981. Sperm isolation and biochemical analysis of the major sperm protein from *Caenorhabditis elegans*. Dev Biol 84:299-312.

Klass, M., Wolf, N., and Hirsh, D. 1976. Development of the male reproductive system and sexual transformation in the nematode *Caenorhabditis elegans*. Dev. Biol. 52:1-18.

Kroft, T. L., Gleason, E. J., and L'Hernault, S. W. 2005. The *spe-42* gene is required for sperm–egg interactions during *C. elegans* fertilization and encodes a sperm specific transmembrane protein. Dev Biol 286:169-181.

LaMunyon, C.W., and Ward, S. 1995. Sperm precedence in a hermaphroditic nematode (*Caenorhabditis elegans*) is due to competitive superiority of male sperm. Experientia 51:817–823.

LaMunyon, C.W., and Ward, S. 1998. Larger sperm outcompete smaller sperm in the nematode *Caenorhabditis elegans*. Proc. R. Soc. Lond. B Biol. Sci. 265:1997–2002.

Lee, D.L. 1971. The structure and development of the spermatozoon of *Heterakis gallinarum*(Nematoda). Journal of Zoology 164:181-187.

Lindsey, W. C. 2002. The *spe-10* and *spe-21* genes encode sperm DHHC-CRD zinc finger proteins required for ER/Golgi membrane morphogenesis during *Caenorhabditis elegans* spermatogenesis. Ph.D. thesis, Emory University, 219 pp.

Lindsey, W. C. and L'Hernault, S. W. 2000. The *spe-10* and *spe-21* genes encode sperm transmembrane proteins that contain a DHHC-CRD zinc finger motif presented in East Coast Worm Meeting.

Lints R, Hall DH. 2006. *Atlas of C elegans Anatomy*: an illustrated handbook. "Male Anatomy." Wormatlas. http://www.wormatlas.org/ver1/handbook/contents.htm.

Liu, K. S., and Sternberg, P. W. 1995. Sensory regulation of male mating behavior in *Caenorhabditis elegans*. Neuron 14:79-89.

L'Hernault, S.W. 1997. Male Germline. In: Riddle D., Blumentahl R., Meyer B.J., and Priess, J. editors. *C. elegans II*. Cold Spring Harbor, NY: Cold Spring Harbor Laboratory Press. 271-294.

L'Hernault, SW. 2009. The genetics and cell biology of spermatogenesis in the nematode *C. elegans.* Mol Cell Endo 306:59–65.

L'Hernault, S. W., and Arduengo, P.M. 1992. Mutation of a putative sperm membrane protein in *Caenorhabditis elegans* prevents sperm differentiation but not its associated meiotic divisions. J Cell Biol 119:55–68.

L'Hernault, S. W., and Roberts, T. M. 1995. Cell biology of nematode sperm. Methods in Cell Biol 48:273-301.

L'Hernault S.W., Shakes D.C., and Ward S. 1988. Developmental genetics of chromosome I spermatogenesis-defective mutants in the nematode *Caenorhabditis elegans*. Genetics 120:435–452.

L'Hernault S.W., and Singson A.W. 2000. Developmental genetics of spermatogenesis in the nematode *Caenorhabditis elegans*. In: Goldberg E., editor. The testes: from stem cell to sperm function, Serono Symposium USA. New York: Springer-Verlag.109-119.

Machaca, K., DeFelice, L.J., and L'Hernault, S.W. 1996. A novel chloride channel localizes to *Caenorhabditis elegans* spermatids and chloride channel blockers induce spermatid differentiation. Dev Biol 176:1–16.

McCarter, J., Bartlett, B., Dang, T. and Schedl, T. 1997. Soma-germ cell interactions in *Caenorhabditis elegans*: multiple events of hermaphrodite germline development require the somatic sheath and spermathecal lineages. Dev Biol 181:121-143.

McCarter J., Bartlett B., Dang T., Schedl T. 1999. On the control of oocyte meiotic maturation and ovulation in *Caenorhabditis elegans*. Dev Biol 205:111–128.

McLaren, D.J. 1973. The structure and development of the spermatozoon of *Dipetalonema viteae* (Nematoda: Filarioidea). Parasitology 66:447-463.

Meyer, B. 1997. Sex determination and X Chromosome dosage compensation**.** In: Riddle, D., Blumentahl, R., Meyer, B.J., and Priess, J. editors. *C. elegans II*. Cold Spring Harbor, NY: Cold Spring Harbor Laboratory Press. 209-240.

Miyamoto, T. 2006. The dendritic cell-specific transmembrane protein DC-STAMP is essential for osteoclast fusion and osteoclast bone-resorbing activity. Mod Rheumatol 16:341–342.

Morgan, D. E., Crittenden, S. L., and Kimble, J. 2010. The *C. elegans* adult male germline: Stem cells and sexual dimorphism. Dev Biol 346:204-214.

Muhlrad P.J., and Ward S. 2002. Spermiogenesis initiation in *Caenorhabditis elegans* involves a casein kinase 1 encoded by the *spe-6* gene. Genetics 161:143–155.

Newman, A. P., White, J. G., and Sternberg, P. W. 1996. Morphogenesis of the *C. elegans* hermaphrodite uterus. Dev 11:3617-3626.

Nelson, G. A., and Ward, S. 1980. Vesicle fusion, pseudopod extension and amoeboid motility are induced in nematode spermatids by the ionophore monensin. Cell 19:457-464.

Nigon, V. 1949. Modalités de la reproduction et déterminsme du sexe chez quelques Nématodes libres. Zool 11:1-32.

Nishimura, H., and L'Hernault, S.W. 2010. Spermatogenesis-defective (*spe*) mutants of the nematode *Caenorhabditis elegans* provide clues to solve the puzzle of male germline functions during reproduction. Developmental Dynamics 239:1502-1514.

O'Brien, T.P., and McCully, M.E. 1969. Plant structure and development: a pictorial and physiological approach. Toronto, Ontario: Macmillan.

Paroutis, P., N. Touret, and S. Grinstein. 2004. The pH of the secretory pathway: measurement, determinants, and regulation. Physiology 19:207–215.

Pavalko, F.M., Roberts, T.M., and Holliday, L.S. 1988. Relationship between plasma membrane mobility and substrate attachment in the crawling movement of spermatozoa from *Caenorhabditis elegans*. Cell Motil Cytoskeleton 11:16–23.

Phillips, C. M., Wong, C., Bhalla, N., Carlton, P. M., Weiser, P., Meneely, P. M., and Dernburg, A. F. 2005. HIM-8 binds to the X chromosome pairing center and mediates chromosome-specific meiotic synapsis. Cell 123:1051-1063.

Reinke V., Smith H.E., Nance J., Wang J., Van Doren C., Begley R., Jones S.J., Davis E.B., Scherer S., Ward S., and Kim S.K. 2000. A global profile of germline gene expression in C. *elegans*. Mol Cell 6:605–616.

Riddle, D. L., Blumenthal, T., Meyer, B. J., and Priess, J. R. 1997. Introduction to *C. elegans*. In D. L. Riddle, T. Blumenthal, B. J. Meyer, and J. R. Priess. Editors. *C. elegans II.* Plainview, NY: Cold Spring Harbor Laboratory Press. 1-6.

Roberts, T.M., Pavalko, F.M., and Ward, S. 1986. Membrane and cytoplasmic proteins are transported in the same organelle complex during nematode spermatogenesis. J. Cell Biol. 102:1787–1796.

Roberts, T. M., and Stewart, M. 1997. Nematode sperm: amoeboid movement without actin. Trends in Cell Biol 7:368-373.

Roberts, T. M., and Ward, S. 1982. Centripetal flow of pseudopodial surface components could propel the amoeboid movement of *Caenorhabditis elegans* spermatozoa. J Cell Biol 92:132-138.

Schedl, T. Germ Line Development 1997. In: Riddle, D., Blumentahl, R., Meyer, B.J., and Priess, J. editors. *C. elegans II*. Cold Spring Harbor, NY: Cold Spring Harbor Laboratory Press. 241-269.

Seidel, H. S., Ailion, M., Li, J., van Oudenaarden, A., Rockman, M. V., and Kruglyak, L.
2011. A novel sperm-delivered toxin causes late-stage embryo lethality and transmission ratio distortion in *C. elegans*. PLoS biology *9*:e1001115.

Seidel, H. S., Rockman, M. V., and Kruglyak, L. 2008. Widespread genetic incompatibility in *C. elegans* maintained by balancing selection. Science 319:589-594.

Seydoux, G., Schedl, T., and Greenwald, I. 1990. Cell-cell interactions prevent a potential inductive interaction between soma and germline in *C. elegans*. Cell 61:939-951.

Shakes, D.C., and Ward, S. 1989a. Initiation of spermiogenesis in *C. elegans*: a pharmacological and genetic analysis. Dev Biol 134:189–200.

Shakes D.C., Ward S. 1989b. Mutations that disrupt the morphogenesis and localization of a sperm-specific organelle in Caenorhabditis elegans. Dev Biol 134:307–316.

Singson, A., Hill, K.L., and L'Hernault, S. W. 1999. Sperm competition in the absence of fertilization in *Caenorhabditis elegans*. Genetics 152:201-208.

Singson, A., Mercer, K.B., and L'Hernault, S.W. 1998. The *C. elegans spe-9* gene encodes a sperm transmembrane protein that contains EGF-like repeats and is required for fertilization. Cell 93:71–79.

Skinner, M.K., Norton, J.N., Mullaney, B.P., Rosselli, M., Whaley, P.D., and Anthony, C.T. 1991. Cell-cell interactions and the regulation of testis function. Ann N.Y Acad Sci 637:354-363.

Smith, H. 2006. Sperm motility and MSP. *WormBook*, ed. The *C. elegans* Research Community, WormBook, doi/10.1895/wormbook.1.68.1, http://www.wormbook.org.

Smith, H.E., and Ward, S. 1998. Identification of protein-protein interactions of the major sperm protein (MSP) of *Caenorhabditis elegans*. J Mol Biol 279:605–619.

Smotrys, J. E., and Linder, M.E. 2004. Palmitoylation of intracellular signaling proteins: regulation and function. Annu Rev Biochem 73: 559–587.

Stanfield, G. M., and Villeneuve, A. M. 2006. Regulation of sperm activation by SWM-1 is required for reproductive success of *C. elegans* Males. Current Biology 16:252-263.

Sulston, J.E., Albertson, D.G., and Thomson, J.N. 1980. The *Caenorhabditis elegans* male: post embryonic development and nongonadal structures. Dev Biol 78:542-576.

Sulston, J.E. 1976. Post-embryonic development in the ventral cord of *Caenorhabditis elegans*. Philos Trans R Soc Lond (Biol) 275:287-297.

Sulston, J.E., and Horvitz, H.R. 1977. Post-embryonic cell lineages in the nematode, *Caenorhabditis elegans*. Dev Biol 56:110-156.

Theriot, J.A. 1996. Worm sperm and advances in cell locomotion. Cell 84:1-4.

Ward, S. 1986. Asymmetric localization of gene products during the development of *Caenorhabditis elegans* spermatozoa. In: Gall, J.G. editor. Gametogenesis and the early embryo. New York: Alan R. Liss, Inc. 55–75.

Ward, S., Argon, Y., and Nelson, G.A. 1981. Sperm morphogenesis in wild-type and fertilization-defective mutants of *Caenorhabditis elegans*. J. Cell Biol. 91:26–44.

Ward S., and Carrel J.S. 1979. Fertilization and sperm competition in the nematode *Caenorhabditis elegans*. Dev Biol 73:304-321.

Ward, S., Hogan, E., and Nelson, G.A. 1983. The initiation of spermiogenesis in the nematode Caenorhabditis elegans. Dev. Biol. 98:70–79.

Ward, S., and Klass, M.1982. The location of the major protein in *Caenorhabditis elegans* sperm and spermatocytes. Dev. Biol. 92:203–208.

White J. 1988. In: The nematode *C. elegans*, W. B. Wood ed. New York: Cold Spring Harbor Laboratory Press. 81-122.

Wilson K.L., Fitch K.R., Bafus B.T., and Wakimoto, B.T. 2006. Sperm plasma membrane breakdown during *Drosophila* fertilization requires sneaky, an acrosomal membrane protein. *Development* 133:4871–4879.

Xu, X.Z., and Sternberg, P.W. 2003. A *C. elegans* sperm TRP protein required for sperm–egg interactions during fertilization. Cell 114:285–297.

Yamada, E. 1957. The fine structure of the megakaryocyte in the mouse spleen. Acta Anat 29: 267-290.

APPENDIX 1

Table 3: Spermatid Diameters and FB-MO Counts for Control and Mutant Genotypes of Interest					
Genotype	**Sex**	**Spermatid Diameter (µm)**	**Number of MOs**	**Ratio Number of MOs: Spermatid Volume (µm^3)**	**Volume(µm^3)**
N2	male	3.5	10	0.4	22
		3.8	14	0.5	28
		3.8	13	0.5	28
		4.3	15	0.4	41
		3.1	11	0.7	16
		4.0	16	0.5	33
		4.3	14	0.3	42
		3.9	15	0.5	31
		5.7	12	0.1	95
		5.6	14	0.2	90
		6.2	12	0.1	124
		6.4	11	0.1	140
		5.4	14	0.2	82
		5.9	14	0.1	105
		5.8	10	0.1	102
		6.1	13	0.1	119
		5.7	11	0.1	99
		5.5	15	0.2	88
		5.4	14	0.2	83
		5.7	16	0.2	99
		5.9	16	0.1	108
		5.7	13	0.1	94
		5.8	16	0.2	100
		5.5	15	0.2	88
		6.3	13	0.1	132
		6.4	14	0.1	137
		5.8	11	0.1	103
		6.8	18	0.1	165
		5.9	15	0.1	109
		5.7	12	0.1	98
		6.3	17	0.1	133
		5.8	16	0.2	100
		5.7	20	0.2	96
		6.8	13	0.1	168
		6.7	17	0.1	157
		6.7	19	0.1	157

Genotype	Sex	Spermatid Diameter (µm)	Number of MOs	Ratio Number of MOs: Spermatid Volume (µm^3)	Volume(µm^3)
N2	male	6.3	15	0.1	131
		7.2	9	0.0	191
		6.7	11	0.1	154
		7.0	12	0.1	181
Genotype	**Sex**	**Average Spermatid Diameter(µm)**	**Average Number of MOs**	**Average Number of MOs: Volume (µm^3)**	**Average Spermatid Volume**
N2	male	5.62	14	0.2	102
	Total n=	**Standard Error Spermatid Diameter**	**Standard Error Number MOs**	**Standard Error Number MOs: Sperm Volume Ratio**	**Standard Error of Average Spermatid Volume**
	40	0.2	0.4	0.02	7.2
Genotype	**Sex**	**Spermatid Diameter (µm)**	**Number of MOs**	**Ratio Number of MOs: Spermatid Volume (µm^3)**	**Volume(µm^3)**
him-5(*e1490*)V	male	4.6	9	0.2	50
		4.9	12	0.2	61
		5.1	14	0.2	69
		5.2	15	0.2	75
		5.7	17	0.2	95
		4.7	6	0.1	54
		4.9	11	0.2	62
		5.4	10	0.1	84
		5.5	12	0.1	88
		5.3	7	0.1	79
		5.3	12	0.2	79
		4.9	11	0.2	60
		4.5	14	0.3	48
		5.1	9	0.1	71
		4.6	8	0.2	52
		4.5	8	0.2	49
		5.3	14	0.2	78
		4.9	15	0.2	63
		5.2	16	0.2	72
		5.1	18	0.3	70
		5.4	13	0.2	81
		5.3	15	0.2	76
		5.6	16	0.2	90
		5.3	13	0.2	78
		4.5	13	0.3	48

Genotype	Sex	Spermatid Diameter (µm)	Number of MOs	Ratio Number of MOs: Spermatid Volume (µm^3)	Volume(µm^3)
him-5(*e1490*)V	male	4.7	16	0.3	55
		5.0	14	0.2	64
		5.8	13	0.1	103
		5.3	11	0.1	76
		5.3	10	0.1	78
Genotype	**Sex**	**Average Spermatid Diameter(µm)**	**Average Number of MOs**	**Average Number of MOs: Volume (µm^3)**	**Average Spermatid Volume**
him-5(*e1490*)V	male	5.1	12	0.2	70
	Total n=	**Standard Error Spermatid Diameter**	**Standard Error Number MOs**	**Standard Error Number of MOs: Sperm Volume Ratio**	**Standard Error of Average Spermatid Volume**
	30	0.1	0.6	0.01	2.6
Genotype	**Sex**	**Spermatid Diameter (µm)**	**Number of MOs**	**Ratio Number MOs: Spermatid Volume (µm^3)**	**Volume(µm^3)**
him-8 (*e1489*)III	male	5.8	15	0.1	103
		5.7	21	0.2	94
		6.3	24	0.2	133
		5.4	17	0.2	82
		6.3	21	0.2	131
		6.3	17	0.1	130
		5.4	17	0.2	81
		5.2	13	0.2	74
		5.3	13	0.2	78
		5.6	14	0.2	93
		4.7	13	0.2	54
		5.1	16	0.2	70
		5.1	10	0.1	69
		5.9	14	0.1	106
		6.0	14	0.1	115
		5.4	17	0.2	84
		6.3	16	0.1	132
		5.6	12	0.1	94
		5.6	17	0.2	93
		5.3	19	0.2	77
		5.6	20	0.2	92

Genotype	Sex	Spermatid Diameter (µm)	Number of MOs	Ratio Number MOs: Spermatid Volume (µm^3)	Volume(µm^3)
him-8 (*e1489*)III	male	6.2	18	0.1	126
		5.6	14	0.1	93
		5.5	19	0.2	87
		5.5	15	0.2	87
		5.8	14	0.1	104
		5.5	15	0.2	87
		5.2	16	0.2	74
		6.4	13	0.1	134
		6.8	8	0.0	168
		6.6	14	0.1	150
		7.0	15	0.1	177
		5.0	14	0.2	66
		5.2	16	0.2	75
		5.2	17	0.2	73
		5.5	14	0.2	88
		5.5	17	0.2	87
		5.1	10	0.1	68
		4.0	11	0.3	34
		5.6	19	0.2	93
		5.6	16	0.2	93
		6.1	18	0.2	119
		7.0	19	0.1	180
		6.7	14	0.1	155
		5.4	13	0.2	84
		5.6	13	0.1	93
		5.5	13	0.2	86
		4.1	8	0.2	36
		5.4	19	0.2	81
		4.9	16	0.3	61
		5.5	14	0.2	86
		5.7	15	0.2	95

Genotype	Sex	Average Spermatid Diameter(µm)	Average Number of MOs	Average Number of MOs: Volume (µm^3)	Average Spermatid Volume
him-8 (*e1489*)III	male	5.6	15	0.2	97
	Total n=	**Standard Error Spermatid Diameter**	**Standard Error Number MOs**	**Standard Error Number MOs: Sperm Volume Ratio**	**Standard Error of Average Spermatid Volume**
	52	0.1	0.4	0.01	4.4
Genotype	**Sex**	**Spermatid Diameter (µm)**	**Number of MOs**	**Ratio Number of MOs: Spermatid Volume (µm^3)**	**Volume(µm^3)**
*fem-3(q23gf)*IV	hermaphrodite	3.6	9	0.4	25
		3.8	10	0.3	29
		4.3	11	0.3	40
		4.0	8	0.2	33
		3.7	6	0.2	27
		3.9	9	0.3	31
		4.1	8	0.2	36
		5.0	14	0.2	66
		5.3	15	0.2	76
		5.2	16	0.2	72
		4.8	13	0.2	58
		4.7	14	0.3	54
		4.4	11	0.2	46
		4.4	14	0.3	46
		5.1	13	0.2	71
		5.6	18	0.2	90
		5.0	18	0.3	65
		5.3	14	0.2	77
		3.6	7	0.3	25
		4.8	9	0.2	59
		5.4	8	0.1	84
		5.4	7	0.1	82
		5.1	12	0.2	70
		5.6	14	0.2	93
		5.6	10	0.1	91
		4.5	11	0.2	46
		4.6	6	0.1	52
		4.7	11	0.2	55
		4.2	8	0.2	40
		5.3	12	0.2	76
		5.1	11	0.2	71

Genotype	Sex	Spermatid Diameter (µm)	Number of MOs	Ratio Number of MOs: Spermatid Volume (µm^3)	Volume(µm^3)
*fem-3(q23gf)*IV	hermaphrodite	4.9	8	0.1	62
		4.2	12	0.3	38
		4.1	13	0.4	35
		3.8	11	0.4	29
		4.2	12	0.3	39
		4.0	14	0.4	34
		4.0	17	0.5	34
		4.4	11	0.2	46
		4.7	13	0.2	54
Genotype	**Sex**	**Spermatid Diameter (µm)**	**Number of MOs**	**Ratio Number of MOs: Spermatid Volume (µm^3)**	**Volume(µm^3)**
*fem-3(q23gf)*IV	hermaphrodite	5.1	15	0.2	70
		4.3	10	0.2	41
		4.1	12	0.3	36
		5.3	11	0.1	78
		4.6	13	0.3	51
		5.8	12	0.1	103
Genotype	**Sex**	**Average Spermatid Diameter(µm)**	**Average Number of MOs**	**Average Number of MOs: Volume (µm^3)**	**Average Spermatid Volume**
*fem-3(q23gf)*IV	hermaphrodite	4.6	12	0.2	55
	Total n=	**Standard Error Spermatid Diameter**	**Standard Error Number of MOs**	**Standard Error Number of MOs: Sperm Volume Ratio**	**Standard Error of Average Spermatid Volume**
	46	0.1	0.4	0.01	3.1
Genotype	**Sex**	**Spermatid Diameter (µm)**	**Number of MOs**	**Ratio Number of MOs: Spermatid Volume (µm^3)**	**Volume(µm^3)**
him-5(e1490)V	hermaphrodite	4.2	8	0.2	39
		3.9	7	0.2	31
		3.8	10	0.4	28
		3.9	8	0.3	31
		4.1	9	0.2	36
		3.7	7	0.3	26
		3.7	9	0.3	27
		3.5	7	0.3	23
		4.6	11	0.2	51
		4.2	10	0.3	39

Genotype	Sex	Average Spermatid Diameter(µm)	Average Number of MOs	Average Number of MOs: Volume (µm^3)	Average Spermatid Volume
him-5(e1490)V	hermaphrodite	4.0	9	0.3	33
	Total Number	**Standard Error Spermatid Diameter**	**Standard Error Number of MOs**	**Standard Error Number of MOs: Sperm Volume Ratio**	**Standard Error of Average Spermatid Volume**
	10	0.1	0.5	0.02	2.68
Genotype	**Sex**	**Spermatid Diameter (µm)**	**Number of MOs**	**Ratio Number of MOs: Spermatid Volume (µm^3)**	**Volume(µm^3)**
spe-8(*hc53*)I	male	5.1	19	0.3	68
		5.1	24	0.4	67
		5.0	21	0.3	64
		5.2	21	0.3	72
		5.3	23	0.3	76
		5.1	18	0.3	69
		5.0	19	0.3	66
		4.9	21	0.3	61
		4.9	17	0.3	63
		5.1	18	0.3	70
		5.1	21	0.3	67
		5.1	19	0.3	69
		4.9	23	0.4	61
		4.8	16	0.3	58
		5.0	17	0.3	64
		5.3	16	0.2	78
		5.2	19	0.3	73
		4.8	18	0.3	59
		4.8	19	0.3	59
		5.2	19	0.3	72
		5.5	18	0.2	86
		5.4	15	0.2	81
		5.5	17	0.2	88
		4.9	16	0.3	63
		4.8	17	0.3	58
		4.8	16	0.3	59
		5.0	17	0.3	64
		5.1	20	0.3	71
		5.5	22	0.2	88
		5.1	20	0.3	71
		4.7	20	0.4	53

Genotype	Sex	Spermatid Diameter (µm)	Number of MOs	Ratio Number of MOs: Spermatid Volume (µm^3)	Volume(µm^3)
spe-8(*hc53*)I	male	5.3	22	0.3	76
		5.3	22	0.3	76
		5.8	18	0.2	102
		5.2	16	0.2	75
		5.9	16	0.2	105
		5.6	18	0.2	94
		5.1	15	0.2	70
		5.8	19	0.2	104
		6.2	17	0.1	126
		5.4	18	0.2	82
		6.1	18	0.2	116
		5.3	17	0.2	78
		5.3	17	0.2	80
		5.6	19	0.2	90
		5.8	15	0.1	102
		5.5	17	0.2	87
		5.9	18	0.2	109
		5.7	17	0.2	95
		5.6	13	0.1	94
		5.5	16	0.2	88
		5.7	19	0.2	95
		5.6	19	0.2	91
		5.8	21	0.2	100
		5.9	18	0.2	105
		5.6	17	0.2	90
		5.2	18	0.2	74
		5.8	19	0.2	103
		5.6	18	0.2	92
		6.0	16	0.1	113
		5.4	18	0.2	80
		4.9	15	0.2	61
		5.9	15	0.1	108
		5.3	17	0.2	76
		5.6	17	0.2	93
		5.5	14	0.2	88
		5.0	13	0.2	64
		6.3	22	0.2	131
		5.7	20	0.2	96
		5.3	13	0.2	76

Genotype	Sex	Spermatid Diameter (µm)	Number of MOs	Ratio Number of MOs: Spermatid Volume (µm^3)	Volume(µm^3)
spe-8(*hc53*)I	male	5.2	18	0.3	72
		5.4	18	0.2	81
		5.5	21	0.2	87
		5.6	17	0.2	93
		5.6	18	0.2	92
		5.4	20	0.2	81
		5.4	17	0.2	81
		5.5	19	0.2	87
		4.9	17	0.3	61
		5.5	21	0.2	87
		5.6	20	0.2	93
		5.4	18	0.2	81
		5.6	16	0.2	93
		5.5	18	0.2	87
		5.9	19	0.2	108
		5.2	18	0.2	75
		5.8	19	0.2	102
		5.5	23	0.3	87
		5.4	18	0.2	81
		5.8	19	0.2	100
		5.2	13	0.2	75
		5.6	18	0.2	90
		5.9	21	0.2	109
		5.8	18	0.2	102
		5.7	16	0.2	95
		5.6	15	0.2	94
		5.6	20	0.2	90
		5.4	22	0.3	81
		5.6	16	0.2	93
		5.9	20	0.2	108
		5.4	12	0.1	81
		5.9	16	0.1	108
		5.4	15	0.2	82
		5.4	17	0.2	83
		6.0	16	0.1	115
		5.1	19	0.3	71
		5.5	13	0.2	87
		4.8	18	0.3	59
		5.5	21	0.2	89

Genotype	Sex	Spermatid Diameter (µm)	Number of MOs	Ratio Number of MOs: Spermatid Volume (µm^3)	Volume(µm^3)
spe-8(*hc53*)I	male	5.7	17	0.2	98
		5.4	15	0.2	84
Genotype	**Sex**	**Average Spermatid Diameter(µm)**	**Average Number of MOs**	**Average Number of MOs: Volume (µm^3)**	**Average Spermatid Volume**
spe-8(*hc53*)I	male	5.4	18	0.2	84
	Total n=	**Standard Error Spermatid Diameter**	**Standard Error Number of MOs**	**Standard Error Number of MOs: Sperm Volume Ratio**	**Standard Error of Average Spermatid Volume**
	111	0.03	0.2	0.01	1.5
Genotype	**Sex**	**Spermatid Diameter (µm)**	**Number of MOs**	**Ratio Number of MOs: Spermatid Volume (µm^3)**	**Volume(µm^3)**
spe-10(*ok1149*)V; *him-8*(*e1489*)IV	male	5.8	16	0.2	100
		6.0	13	0.1	115
		5.5	16	0.2	87
		5.7	14	0.1	95
		5.9	18	0.2	108
		5.8	19	0.2	100
		5.7	13	0.1	97
		5.5	13	0.2	87
		5.6	14	0.2	92
		6.0	12	0.1	115
		6.4	15	0.1	139
		5.6	12	0.1	94
		6.3	17	0.1	132
		6.7	20	0.1	154
		5.6	15	0.2	93
		6.3	17	0.1	132
		5.9	18	0.2	108
		6.5	15	0.1	142
		6.7	14	0.1	157
		6.3	14	0.1	133
		5.4	11	0.1	82
		5.8	11	0.1	100
		6.4	13	0.1	134
		6.5	13	0.1	142
		6.7	17	0.1	154
		5.9	16	0.1	108

Genotype	Sex	Spermatid Diameter (µm)	Number of MOs	Ratio Number of MOs: Spermatid Volume (µm^3)	Volume(µm^3)
spe-10(*ok1149*)V; *him-8*(*e1489*)IV	male	6.3	18	0.1	131
		5.9	15	0.1	108
		5.7	12	0.1	97
		6.6	21	0.1	148
		5.9	15	0.1	109
		5.8	13	0.1	104
		6.2	19	0.2	124
		6.4	16	0.1	135
		5.8	15	0.1	100
		5.9	17	0.2	108
		6.2	16	0.1	127
		7.0	16	0.1	180
		6.0	18	0.2	115
		5.3	11	0.1	76
		5.6	12	0.1	94
		6.3	15	0.1	130
		6.8	14	0.1	168
		5.2	14	0.2	73
		6.6	14	0.1	148
		6.0	15	0.1	110
		6.3	14	0.1	131
		5.4	16	0.2	82
		6.5	15	0.1	142
		6.5	17	0.1	144
		6.4	13	0.1	137
		5.6	17	0.2	92
		6.4	19	0.1	137
		5.7	11	0.1	95
		6.0	15	0.1	115
		5.3	14	0.2	78
		6.4	18	0.1	140
		6.5	19	0.1	144
		6.6	19	0.1	148
		6.4	16	0.1	135

Genotype	Sex	Average Spermatid Diameter(µm)	Average Number of MOs	Average Number of MOs: Volume (µm^3)	Average Spermatid Volume
spe-10(*ok1149*)V; *him-8*(*e1489*)IV	male	6.1	15	0.1	118
	Total n=	**Standard Error Spermatid Diameter**	**Standard Error Number of MOs**	**Standard Error Number of MOs: Sperm Volume Ratio**	**Standard Error of Average Spermatid Volume**
	60	0.1	0.3	0.004	3.2
Genotype	**Sex**	**Spermatid Diameter (µm)**	**Number of MOs**	**Ratio Number of MOs: Spermatid Volume (µm^3)**	**Volume(µm^3)**
spe-21(*hc113*)III; *him-5*(*e1490*)V	male	5.1	8	0.1	68
		4.6	12	0.2	50
		4.7	9	0.2	54
		4.5	9	0.2	48
		4.2	8	0.2	39
		4.8	11	0.2	58
		4.4	11	0.3	44
		4.0	8	0.2	34
		5.0	11	0.2	66
		4.5	11	0.2	49
		4.7	10	0.2	53
		4.4	8	0.2	46
		5.1	12	0.2	70
		4.6	10	0.2	51
		5.0	10	0.2	65
		4.7	9	0.2	54
		4.9	11	0.2	61
		3.7	8	0.3	26
		4.0	8	0.2	34
		5.1	9	0.1	70
		4.0	7	0.2	34
		5.0	8	0.1	65
		4.5	10	0.2	47
		4.8	8	0.1	57
		4.6	6	0.1	49
		4.6	7	0.1	52
		5.2	8	0.1	72
		4.7	6	0.1	53

Genotype	Sex	Spermatid Diameter (µm)	Number of MOs	Ratio Number of MOs: Spermatid Volume (µm^3)	Volume(µm^3)
spe-21(*hc113*)III; *him-5*(*e1490*)V	male	4.9	7	0.1	61
		4.8	9	0.2	59
Genotype	**Sex**	**Average Spermatid Diameter(µm)**	**Average Number of MOs**	**Average Number of MOs: Volume (µm^3)**	**Average Spermatid Volume**
spe-21(*hc113*)III; *him-5*(*e1490*)V	male	4.6	9.0	0.2	53
	Total n=	**Standard Error Spermatid Diameter**	**Standard Error Number of MOs**	**Standard Error Number of MOs: Sperm Volume Ratio**	**Standard Error of Average Spermatid Volume**
	30	0.1	0.3	0.01	2.2
Genotype	**Sex**	**Spermatid Diameter (µm)**	**Number of MOs**	**Ratio Number of MOs: Spermatid Volume (µm^3)**	**Volume(µm^3)**
spe-42(*tm2421*)V; *him-8*(*e1489*)IV	male	4.3	9	0.2	42
		4.6	8	0.2	52
		4.4	10	0.2	46
		4.4	9	0.2	43
		4.5	8	0.2	47
		4.6	9	0.2	50
		3.9	7	0.2	31
		4.5	12	0.3	47
		4.3	10	0.2	43
		4.3	13	0.3	40
		4.5	12	0.3	46
		4.1	9	0.2	37
		4.6	10	0.2	52
		4.1	8	0.2	36
		4.3	11	0.3	40
		4.5	10	0.2	46
		4.1	10	0.3	37
		4.2	11	0.3	39
		4.2	10	0.3	38
		4.3	9	0.2	40
		4.2	12	0.3	39
		4.2	7	0.2	39

Genotype	Sex	Spermatid Diameter (µm)	Number of MOs	Ratio Number of MOs: Spermatid Volume (µm^3)	Volume(µm^3)
spe-42(*tm2421*)V; *him-8*(*e1489*)IV	male	4.3	14	0.3	43
		5.1	16	0.2	69
		3.7	9	0.3	26
		4.1	12	0.3	37
		4.2	17	0.4	39
		3.9	10	0.3	32
		4.1	11	0.3	35
		4.1	9	0.3	35
		4.2	13	0.3	38
		4.0	10	0.3	33
		4.2	11	0.3	39
		3.8	8	0.3	29
		4.9	12	0.2	61
		4.2	9	0.2	40
		5.2	8	0.1	75
		4.9	9	0.1	62
		5.2	11	0.2	72
		4.4	8	0.2	45
		5.5	9	0.1	86
		5.7	15	0.2	94
		5.5	11	0.1	88
		5.4	13	0.2	83
		5.6	9	0.1	92
		5.7	14	0.1	97
		5.2	13	0.2	72
		5.4	15	0.2	81
		5.3	10	0.1	79
		5.7	17	0.2	97
		5.4	10	0.1	82
		5.4	12	0.1	83

Genotype	Sex	Average Spermatid Diameter(µm)	Average Number of MOs	Average Number of MOs: Volume (µm^3)	Average Spermatid Volume
spe-42(*tm2421*)V; *him-8*(*e1489*)IV	male	4.6	11	0.2	53
	Total n=	**Standard Error Spermatid Diameter**	**Standard Error Number of MOs**	**Standard Error Number of MOs: Sperm Volume Ratio**	**Standard Error of Average Spermatid Volume**
	52	0.1	0.3	0.01	2.9
Genotype	**Sex**	**Spermatid Diameter (µm)**	**Number of MOs**	**Ratio Number of MOs: Spermatid Volume (µm^3)**	**Volume(µm^3)**
fer-14(*ok2070*)I; *him-5*(*e1490*)V	male	6.3	18	0.1	131
		5.8	14	0.1	102
		6.0	18	0.2	113
		5.7	20	0.2	97
		6.2	19	0.2	123
		5.8	16	0.2	101
		6.0	20	0.2	114
		5.9	16	0.2	105
		5.6	15	0.2	93
		5.5	19	0.2	88
		6.4	19	0.1	139
		5.8	14	0.1	101
		5.4	16	0.2	82
		5.6	16	0.2	90
		5.2	16	0.2	75
		5.4	16	0.2	81
		5.6	19	0.2	93
		6.2	21	0.2	123
		5.7	16	0.2	99
		4.8	11	0.2	59
		6.1	22	0.2	116
		5.4	17	0.2	82
		5.8	17	0.2	103
		5.6	17	0.2	93
		5.2	19	0.3	75
		5.9	21	0.2	108
		5.4	14	0.2	82
		5.5	22	0.3	87

		5.9	19	0.2	107
		5.9	21	0.2	108
		5.9	19	0.2	106
		5.3	16	0.2	76
		5.7	17	0.2	95
		5.3	17	0.2	78
		5.5	17	0.2	85
		5.6	20	0.2	92
		5.9	17	0.2	108
		6.1	20	0.2	119
		5.9	18	0.2	108
		5.8	17	0.2	101
		5.6	16	0.2	90
		5.7	15	0.2	94
Genotype	**Sex**	**Average Spermatid Diameter(µm)**	**Average Number of MOs**	**Average Number of MOs: Volume (µm^3)**	**Average Spermatid Volume**
fer-14(*ok2070*)I; *him-5*(*e1490*)V	male	5.7	18	0.2	98
	Total n=	**Standard Error Spermatid Diameter**	**Standard Error Number of MOs**	**Standard Error Number of MOs: Sperm Volume Ratio**	**Standard Error of Average Spermatid Volume**
	42	0.05	0.4	0.004	2.5
Genotype	**Sex**	**Spermatid Diameter (µm)**	**Number of MOs**	**Ratio Number of MOs: Spermatid Volume (µm^3)**	**Volume(µm^3)**
peel-1(*qq99*)I	male	5.4	26	0.3	81
		4.2	17	0.5	38
		3.9	13	0.4	31
		4.1	18	0.5	36
		3.9	18	0.6	31
		6.3	22	0.2	132
		6.1	20	0.2	119
		6.1	20	0.2	120
		6.0	17	0.2	111
		6.2	20	0.2	124
		5.2	18	0.3	72
		5.3	18	0.2	79
		6.1	20	0.2	119
		5.6	22	0.2	90
		6.2	21	0.2	123
		5.8	20	0.2	101

Genotype	Sex	Spermatid Diameter (µm)	Number of MOs	Ratio Number of MOs: Spermatid Volume (µm^3)	Volume(µm^3)
peel-1(*qq99*)I	male	6.0	19	0.2	114
		5.5	19	0.2	85
		5.5	15	0.2	85
		5.5	14	0.2	86
		5.8	23	0.2	102
		5.5	18	0.2	87
		5.8	21	0.2	100
		5.4	17	0.2	81
		5.8	16	0.2	102
		5.4	17	0.2	82
		5.8	24	0.2	103
		5.9	18	0.2	107
		5.8	16	0.2	100
		5.8	16	0.2	100
		5.3	15	0.2	77
		6.7	25	0.2	155
		5.8	18	0.2	102
		5.9	19	0.2	108
		6.1	21	0.2	120
		5.9	17	0.2	109
		6.5	27	0.2	144
		5.7	15	0.2	95
		6.0	19	0.2	115
		6.3	20	0.2	128
Genotype	**Sex**	**Average Spermatid Diameter(µm)**	**Average Number of MOs**	**Average Number of MOs: Volume (µm^3)**	**Average Spermatid Volume**
peel-1(*qq99*)I	male	5.6	19	0.2	97
	Total n=	**Standard Error Spermatid Diameter**	**Standard Error Number of MOs**	**Standard Error Number of MOs: Sperm Volume Ratio**	**Standard Error of Average Spermatid Volume**
	40	0.1	0.5	0.02	4.5

Genotype	Sex	Spermatid Diameter (µm)	Number of MOs	Ratio Number of MOs: Spermatid Volume (µm^3)	Volume(µm^3)
N2	hermaphrodite	4.1	6	0.2	37
		4.2	5	0.1	37
		3.9	8	0.3	31
		4.2	5	0.1	38
		3.8	5	0.2	29
		4.1	6	0.2	35
		3.9	5	0.2	32
		3.5	4	0.2	22
Genotype	**Sex**	**Average Spermatid Diameter(µm)**	**Average Number of MOs**	**Average Number of MOs: Volume (µm^3)**	**Average Spermatid Volume**
N2	hermaphrodite	3.9	6	0.2	33
	Total n=	**Standard Error Spermatid Diameter**	**Standard Error Number of MOs**	**Standard Error Number of MOs: Sperm Volume Ratio**	**Standard Error of Average Spermatid Volume**
	8	0.1	0.4	0.01	1.9
*alternating blue and white rows indicate results from different animals that were dissected					